

AD A 040 537

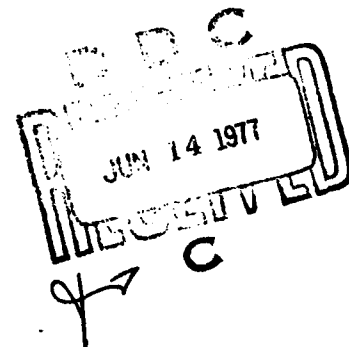
## Description and Use of the Plume Radiation Code ATLES

12  
NW

Chemistry and Physics Laboratory ✓  
Laboratory Operations  
The Ivan A. Getting Laboratories  
El Segundo, Calif. 90245

18 May 1977

Interim Report



APPROVED FOR PUBLIC RELEASE;  
DISTRIBUTION UNLIMITED

Sponsored by  
DEFENSE ADVANCED RESEARCH PROJECTS AGENCY (DOD)  
DARPA Order No. 2843  
Monitored by SAMSO under Contract No. F04701-76-C-0077

SPACE AND MISSILE SYSTEMS ORGANIZATION  
AIR FORCE SYSTEMS COMMAND  
Los Angeles Air Force Station  
P.O. Box 92960, Worldway Postal Center  
Los Angeles, Calif. 90009


AD NO. \_\_\_\_\_  
DDC FILE COPY.


THE VIEWS AND CONCLUSIONS CONTAINED IN THIS DOCUMENT ARE THOSE  
OF THE AUTHORS AND SHOULD NOT BE INTERPRETED AS NECESSARILY  
REPRESENTING THE OFFICIAL POLICIES, EITHER EXPRESSED OR IMPLIED, OF  
THE DEFENSE ADVANCED RESEARCH PROJECTS AGENCY OR THE U.S.  
GOVERNMENT.

This report was submitted by The Aerospace Corporation, El Segundo, CA 90245, under Contract F04701-76-C-0077 with the Space and Missile Systems Organization, P. O. Box 92960, Worldway Postal Center, Los Angeles, CA 90009. It was reviewed and approved for The Aerospace Corporation by S. Siegel, Director, Chemistry and Physics Laboratory. Lt. A. G. Fernandez, SAMSO/YAPT, was the project officer. This research was supported by the Defense Advanced Research Projects Agency of the Department of Defense.


This report has been reviewed by the Information Office (OI) and is releasable to the National Technical Information Service (NTIS). At NTIS, it will be available to the general public, including foreign nations.

This technical report has been reviewed and is approved for publication.

  
ARTURO G. FERNANDEZ, Lt, USAF  
Project Officer

  
JOSEPH GASSMANN, Maj, USAF

FOR THE COMMANDER

  
FLOYD R. STUART, Colonel, USAF  
Deputy for Advanced Space Programs

Handwritten signature: *A*

Stamp: *RECEIVED*

Stamp: *DEFENSE ADVANCED RESEARCH PROJECTS AGENCY*

Stamp: *WASHINGTON, D.C.*

Stamp: *1976*

Stamp: *1*

UNCLASSIFIED

SECURITY CLASSIFICATION OF THIS PAGE (When Data Entered)

REPORT DOCUMENTATION PAGE		READ INSTRUCTIONS BEFORE COMPLETING FORM
1. REPORT NUMBER SAMS0 TR-77-100	2. GOVT ACCESSION NO.	3. RECIPIENT'S CATALOG NUMBER
4. TITLE (and Subtitle) DESCRIPTION AND USE OF THE PLUME RADIATION CODE ATLES	5. TYPE OF REPORT & PERIOD COVERED Interim rept.	6. PERFORMING ORG. REPORT NUMBER TR-0077 (2753-04)-3
7. AUTHOR(s) Stephen J. Young	8. CONTRACT OR GRANT NUMBER(s) F04701-76-C-0077 Dit-A Ord-r-2243	9. PROGRAM ELEMENT, PROJECT, TASK AREA & WORK UNIT NUMBERS
10. PERFORMING ORGANIZATION NAME AND ADDRESS The Aerospace Corporation El Segundo, Calif. 90245	11. CONTROLLING OFFICE NAME AND ADDRESS Defense Advanced Research Projects Agency 1400 Wilson Blvd. Arlington, Va. 22209	12. REPORT DATE 13 May 1977
13. MONITORING AGENCY NAME & ADDRESS (if different from Controlling Office) Space and Missile Systems Organization Air Force Systems Command Los Angeles, Calif. 90045	14. NUMBER OF PAGES 100	15. SECURITY CLASS. (of this report) Unclassified
16. DISTRIBUTION STATEMENT (of this Report) Approved for public release; distribution unlimited.		15a. DECLASSIFICATION/DOWNGRADING SCHEDULE
17. DISTRIBUTION STATEMENT (of the abstract entered in Block 20, if different from Report)		
18. SUPPLEMENTARY NOTES		
19. KEY WORDS (Continue on reverse side if necessary and identify by block number) Rocket Exhaust Plumes Infrared Radiation Target Signature Code		
20. ABSTRACT (Continue on reverse side if necessary and identify by block number) The computer code ATLES is designed to compute the infrared radiance signatures of missile and aircraft exhaust plumes with allowance for attenuation by arbitrary atmospheric slant paths. The code is significantly improved over existing radiation codes through the use of newly developed band radiation formulations for nonuniform optical paths and the use of temperature-consistent band model parameters. Descriptions of the radiation formulation and some of the significant computational routines are presented. The latter include the geometry of intersection between an arbitrary line of sight		

UNCLASSIFIED

SECURITY CLASSIFICATION OF THIS PAGE(When Data Entered)

19. KEY WORDS (Continued)

20. ABSTRACT (Continued)

through the atmosphere and a plume contained within a paraboloid control volume. Detailed instructions on the preparation of input data are presented, and use of the code is illustrated by an application to a jet-aircraft plume.

UNCLASSIFIED

## CONTENTS

I.	INTRODUCTION .....	5
II.	RADIATION MODEL .....	11
	A. Introduction .....	11
	B. Radiance Calculation .....	13
	C. y-Functions for Lorentz Line Shape .....	15
	D. y-Functions for Doppler Line Shape .....	19
	E. y-Function for Voigt Line Shape .....	25
III.	COMPUTER CODE ATLES .....	27
	A. Flow Diagram .....	27
	B. Subroutine MODATM .....	35
	C. Subroutine VIEW .....	36
	D. Subroutine SPATH .....	41
	E. Subroutine DELTRAN .....	52
IV.	PREPARATION OF INPUT DATA .....	55
	A. Title Card .....	55
	B. Calculation Mode Card .....	55
	C. Path Intervals Card .....	57
	D. Inhomogeneity Approximations Card .....	58
	E. Spectrum Card .....	59
	F. Bandpass Card .....	60
	G. Geometry Card .....	60
	H. Print Cards .....	61
	I. Plot Card .....	61
	J. Species Card .....	63
	K. Atmosphere Card .....	63
	L. Source Card .....	67
	M. Plume Integration Card .....	69
	N. Execution Card .....	74

## CONTENTS (Continued)

V.	EXAMPLE CALCULATIONS .....	77
A.	ERIM Hot-through-Cold H <sub>2</sub> O Spectra .....	77
B.	J57 - Jet-Engine Plume .....	80
VI.	CODE DISTRIBUTION .....	97
	REFERENCES .....	99

## FIGURES

1.	Schematic Coupled Path Geometry. . . . .	12
2.	ATLES Flow Diagram . . . . .	28
3.	Atmospheric Slant Path Geometry for a Sensor above the Atmosphere . . . . .	37
4.	Atmospheric Slant Path Geometry for a Sensor within the Atmosphere . . . . .	39
5.	Geometry of Intersection between an Optical Line of Sight and Paraboloid Plume Control Surface . . . . .	42
6.	General Intersection Cases . . . . .	43
7.	Axial Coordinate Test Points . . . . .	45
8.	Intermediate Interpolation for Case 1. . . . .	49
9.	Interpolation Surface. . . . .	50
10.	Case 2 Interpolation Geometry . . . . .	51
11.	Program Control Card Formats . . . . .	56
12.	Band Model Parameter Set Deck Structure . . . . .	64
13.	Deck Structure for Model Atmosphere Input Data . . . . .	66
14.	Deck Structure for Emission or Absorption Cell Input Data . . . . .	68
15.	Deck Structure for Plume Input Data . . . . .	70
16.	Deck Structure for Integration Grid Input Data. . . . .	72
17.	Control Card and Auxiliary Data Input Deck for ERIM Hot-through Cold H <sub>2</sub> O Spectra . . . . .	78
18.	Output Listing for ERIM Case 9R with DR Approximation . . . . .	81
19.	Comparison of Computed and Experimental Radiance Spectra for ERIM Hot-through Cold H <sub>2</sub> O Measurements . . . . .	82

## FIGURES (Continued)

20.	Plume Temperature Profiles . . . . .	83
21.	Plume Concentration Profiles . . . . .	84
22.	Input Data Deck Listing for Jet-Plume Calculation Runs . . . . .	85
23.	Projected Area Integration Grid . . . . .	88
24.	Output Listing for Jet-Plume Calculation in the 4.3- $\mu$ m Region with Aircraft-Sensor Geometry . . . . .	89
25.	Radiance Spectra in 2.7- $\mu$ m Region . . . . .	91
26.	Radiance Spectra in 4.3- $\mu$ m Region . . . . .	92
27.	Atmospheric and Effective Atmospheric Transmittance Spectra . . . . .	93
28.	Axial-Station Variation of the 4.3- $\mu$ m Blue Spike Radiance for Aircraft-Sensor Geometry . . . . .	94
29.	Isoradiance Contours of the 4.3- $\mu$ m Blue Spike Radiance for Aircraft-Sensor Geometry . . . . .	95

## TABLES

1.	Model Atmosphere File . . . . .	7
2.	Band Model Parameter File . . . . .	8
3.	Curve of Growth Functions for Statistical Doppler Line Band Model . . . . .	21
4.	Equivalent Width Derivative Function for Statistical Doppler Line Band Model . . . . .	24
5.	LOS - Plume Intersection Cases . . . . .	46



## I. INTRODUCTION

The computer code ATLES\* and its associated subprograms and data bases are designed to perform band model calculations of the infrared radiance signatures of missile and aircraft exhaust plumes at arbitrary altitude as viewed through arbitrary atmospheric slant paths. The code is significantly improved over previous codes through the use of newly-developed band radiation formulations for highly-nonuniform optical paths and the use of temperature-consistent band model parameters for  $H_2O$  and  $CO_2$ .

The band radiation model is formulated within the statistical band model for Lorentz line shape with approximate corrections made for Doppler broadening effects. Thus, the model can be applied to plume problems involving arbitrary target and sensor altitudes. An optical line of sight from a sensor, through the absorbing atmosphere, and through a chord of an exhaust plume is handled as a coupled optical path so that line correlation between the plume-emission and atmospheric-absorption spectra is correctly treated. Line correlation is important whenever the plume and atmosphere contain molecular species in common (e.g.,  $H_2O$  or  $CO_2$ ). Optical path nonuniformities caused by this coupling approach are generally too large to be handled accurately by the traditional Curtis-Godson approximation. For such coupled paths, more sophisticated approximations have been developed and are employed in ATLES. Complete descriptions of the radiation models are given in Section II.

In its most general computational mode, ATLES computes the spectral and spatial distributions of radiance (both unattenuated and attenuated by the intervening atmosphere) over the projected area of a plume for arbitrary viewing aspect angle. Calculation options allow integration of the radiance distributions over spectral bandpasses to

---

\*ATLES is an acronym for Atmospheric Transmittance to Line Emission Sources and is meant to be pronounced as atlas.

get inband radiance values and/or spatial integrations over the projected area of a plume to get axial-station variations or whole plume averages. The ratio of the attenuated to the unattenuated whole plume radiance spectra defines an "effective" atmospheric transmittance which, because of line correlation effects, will generally not be the same as that obtained by traditional atmospheric transmittance codes.<sup>(1)</sup> The latter codes predict attenuation factors for continuum radiation only, or for emission and absorption by dissimilar species. Although the primary emphasis of the calculational routines of ATLES is directed toward the plume-atmosphere problem, subsidiary calculation modes can be selected to simulate laboratory cell and flame radiation measurements.

Primary inputs to the code are the distribution of pressure, temperature, and species concentration data (pTc data) within the exhaust plume, pTc altitude profiles for the atmosphere, and band model parameters for the molecular species of the plume and atmosphere. The specification of pTc data for the plume is strictly a user's responsibility. No data base of plume models is maintained for use in ATLES. Band model parameters and model atmospheres may be user specified also; but data bases of parameters and atmospheres have been constructed specifically for use with ATLES.

The model atmosphere data base (Table 1) contains six familiar standard atmospheres.<sup>(2)</sup>

The band model parameter data base contains parameters for  $H_2O$ ,  $CO_2$ ,  $CO$ ,  $HF$ ,  $HCl$  and  $H_2O$ . Spectral regions and resolutions for these various parameter sets are given in Table 2. Parameter sets whose identification name is prefixed by NASA were constructed from the tabulation of Ludwig, et al.<sup>(3)</sup> The prefix LINAVE denotes parameter sets derived from the AFGL atmospheric absorption line data compilation.<sup>(4)</sup> Treatment of the plume and atmosphere in a coupled manner requires that the band model parameters used in the radiation model be consistent in the temperature range from atmospheric values ( $\sim 200^\circ K$ ) to gas combustion ( $\sim 3000^\circ K$ ) values. For  $H_2O$  and  $CO_2$ , the NASA parameters

Table 1. Model Atmosphere File

Section Number	Identification Name	Atmospheric Model
1	MCCTROPICL	Tropical
2	MCCMIDLATS	Midlatitude Summer
3	MCCMIDLATW	Midlatitude Winter
4	MCCSUBARCS	Subarctic Summer
5	MCCSUBARCW	Subarctic Winter
6	US1962	U. S. 1962 Standard

Table 2. Band Model Parameter File

Section Number	Identification Name	Species	Spectral Data ( $\text{cm}^{-1}$ )				Temperature Range ( $^{\circ}\text{K}$ )
			$\nu_{\text{min}}$	$\nu_{\text{max}}$	Increment	$\Delta\nu$	
1	COMBH2O	H <sub>2</sub> O	2500	4500	25	25	100-3000
2	COMBCO2A	CO <sub>2</sub>	2000	2400	5	5	100-3000
3	COMBCO2B	CO <sub>2</sub>	2000	2415	5	25	100-3000
4	COMBCO2C	CO <sub>2</sub>	3100	3770	5	5	100-3000
5	COMBCO2D	CO <sub>2</sub>	3100	3785	5	25	100-3000
6	LINAVEN2OA	N <sub>2</sub> O	1715	2625	5	5	100-3000*
7	LINAVEN2OB	N <sub>2</sub> O	1705	2635	5	25	100-3000*
8	NASACO	CO	1100	2350	25	~25	300-3000†
9	NASAHCL	HCl	1000	3225	variable	~25	300-3000†
10	NASAHF	HF	1400	4450	variable	~25	300-3000†

\* Meaningful only for  $T \lesssim 500^{\circ}\text{K}$ .† Extrapolation used for  $T < 300^{\circ}\text{K}$ .

have been shown to be inadequate for low-temperature application and the LINAVE parameters inadequate for high-temperature application.<sup>(5, 6)</sup> The latter inadequacy results from the lack of hot line data in the AFGL compilation. For the reverse application, the two parameter sets are quite adequate. The prefix COMB denotes parameter sets that have been constructed<sup>(5, 6)</sup> by combining the low-temperature LINAVE and high-temperature NASA parameters in order to get temperature-consistent parameter sets. Nominal usage considers H<sub>2</sub>O, CO<sub>2</sub>, CO, HF, or HCl as possible plume radiation species and H<sub>2</sub>O, CO<sub>2</sub>, CO, or N<sub>2</sub>O as possible atmospheric absorption species.

This report is both a description of and user's guide for the plume radiation code ATLES. The band radiation formulation is described in Section II. A brief discussion of the calculation procedures of ATLES is given in Section III. A detailed description of input data preparation is contained in Section IV. Familiarity with the contents of Sections II and III on the description of the code is not crucial to data preparation or use of the code. Example applications of the code are given in Section V, and information on distribution of the code to interested users is given in Section VI.

## II. RADIATION MODEL

### A. Introduction

Radiation calculations in ATLES are performed entirely within the statistical band model formulation with an inverse or exponential-tailed inverse line strength distribution. Derivations and discussions of the basic models and approximations that account for nonuniformities along optical paths and Doppler broadening effects are given in Refs. 7 through 10. Only the equations defining the models and methods of calculation are given here. In general, the optical path considered is a highly-nonuniform path consisting of a cool absorption path coupled to a hot emission path with common molecular species in each path segment. The terms "absorption path" and "emission" path are identification names only, since any optical path both absorbs and emits radiation. The names identify the dominant radiation phenomenon associated with each path in the context of the present problem. The absorption path may represent either an atmospheric slant path or laboratory absorption cell, while the emission path may represent a line of sight through an exhaust plume or a laboratory flame or hot-gas cell. A schematic diagram of a coupled optical path is shown in Figure 1. This diagram is meant to convey the impression that the optical path is nonuniform both through gradients in the absorption and emission path segments, and through the fact that the segments are treated in a coupled manner. Treatment in a coupled manner is mandatory when active species are common in both the absorption and emission path segments. The high degree of line position correlation between the monochromatic emission and absorption spectra precludes decoupling the total optical path into its component segments and computing the radiance spectra at the sensor position as the product of the emission path radiance and absorption path transmittance. Depending on the degree of nonuniformity within the emission path segment, such a procedure could yield a sensor radiance that is larger or smaller than the true radiance, and only fortuitously the same.

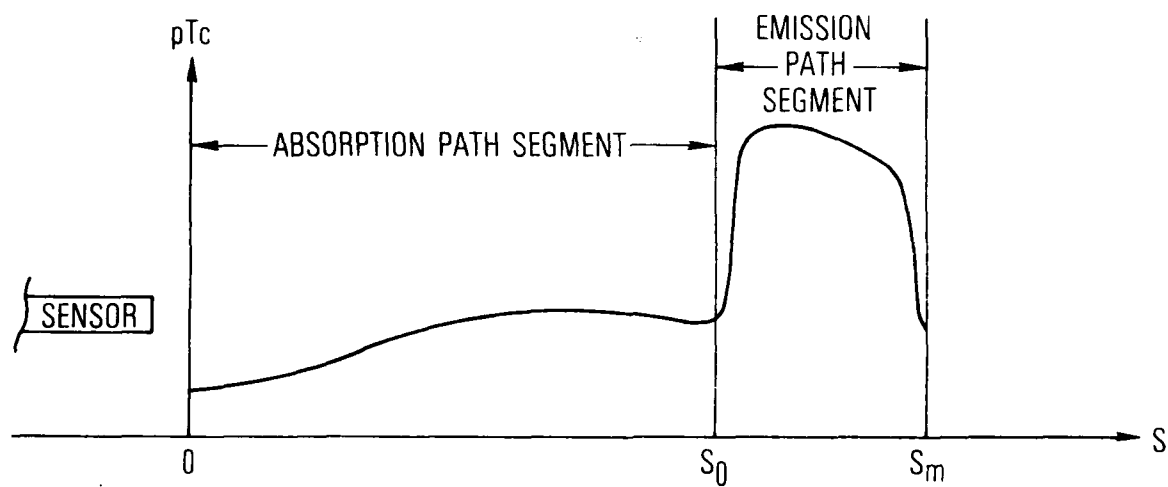


Figure 1. Schematic Coupled Path Geometry.

The following radiation band models are applicable to any non-uniform optical path along which the pressure  $p(s)$ , temperature  $T(s)$ , and concentration of active species  $c(s)$  is known as a function of path position  $s$ . The total length is  $s_m$  and the sensor is located at  $s = 0$ . It is assumed that no radiation source exists beyond  $s = s_m$ . The band model parameters  $\bar{k}(s)$ ,  $\bar{\delta}(s)$ , and  $\bar{\gamma}(s)$  are presumed known along the path through  $p(s)$ ,  $T(s)$ , and  $c(s)$ .

#### B. Radiance Calculation

The mean value of radiance in an interval  $\Delta\nu$  around  $\nu$  is given by

$$\bar{N} = - \int_0^{s_m} N^*(s) \frac{d\bar{\tau}(s)}{ds} ds \quad (1)$$

where  $N^*(s)$  is the Planck radiation function evaluated at temperature  $T(s)$  and wavenumber  $\nu$ .  $\bar{\tau}(s)$  is the mean transmittance in  $\Delta\nu$  for the path between  $s = 0$  and general position  $s$  caused by all active molecular species. It is axiomatic within the statistical model that the total transmittance due to several species is the product of the transmittances for each species. Thus

$$\bar{\tau}(s) = \prod_j \bar{\tau}_j(s) \quad (2)$$

and

$$\frac{d\bar{\tau}(s)}{ds} = \bar{\tau}(s) \sum_j \frac{1}{\bar{\tau}_j(s)} \frac{d\bar{\tau}_j(s)}{ds} \quad (3)$$

can be used to compute  $\bar{\tau}(s)$  and  $d\bar{\tau}(s)/ds$  once the transmittance and transmittance derivative for each species are known. The remaining discussion is limited to one species, and the subscript  $j$  is suppressed.



Within the form of the statistical model used here, the mean transmittance is given by

$$\bar{\tau}(s) = e^{-\frac{\bar{W}(s)}{\delta}} \quad (4)$$

where  $\bar{W}(s)/\delta$  is an equivalent width function. The transmittance derivative is

$$\frac{d\bar{\tau}(s)}{ds} = -\bar{\tau}(s) \frac{1}{\delta} \frac{d\bar{W}(s)}{ds} \quad (5)$$

For all line shapes and inhomogeneity approximations, the equivalent width derivative is given by

$$\frac{1}{\delta} \frac{d\bar{W}(s)}{ds} = c(s) p(s) \bar{k}(s) y(s) \quad (6)$$

where only the function  $y(s)$  changes with the model. The following sections deal with this  $y$ -function. When  $y(s)$  has been determined as a function of  $s$ , and thus also the equivalent width derivative by Eq. (6), the equivalent width is determined by integration

$$\frac{\bar{W}(s)}{\delta} = \int_0^s \frac{1}{\delta} \frac{d\bar{W}(s')}{ds'} ds' \quad (7)$$

or, in the case of the CG approximation, by formula [Eq. (18) or (43)]. Then, Eq. (4) can be used to obtain  $\bar{\tau}(s)$ , and Eq. (5) to get  $d\bar{\tau}(s)/ds$ . Once  $\bar{\tau}(s)$  and  $d\bar{\tau}(s)/ds$  are known for all species, Eqs. (2) and (3) are used to obtain the total transmittance and derivative and Eq. (1) used to obtain  $\bar{N}$ .

C. y-Functions for Lorentz Line Shape

Three models of the y-function for Lorentz lines are included in ATLES. The CG approximation is

$$y(s) = y[\pi x(s), \rho(s)] \quad (8)$$

where

$$y(\eta, \rho) = (2 - \rho) \frac{dI(\eta)}{d\eta} + (\rho - 1) \frac{I(\eta)}{\eta} \quad (9)$$

with

$$I(\eta) = \sqrt{1 + 2\eta} - 1 \quad (10)$$

$$\frac{dI(\eta)}{d\eta} = \frac{1}{\sqrt{1 + 2\eta}} \quad (11)$$

$$x(s) = \frac{u(s) \bar{k}_e(s)}{\beta_e(s)} \quad (12)$$

$$\rho(s) = \frac{\beta(s)}{\beta_e(s)} \quad (13)$$

$$u(s) = \int_0^s c(s') p(s') ds' \quad (14)$$

$$\bar{k}_e(s) = \frac{1}{u(s)} \int_0^s c(s') p(s') \bar{k}(s') ds' \quad (15)$$

$$\beta_e(s) = \frac{1}{u(s) \bar{k}_e(s)} \int_0^s c(s') p(s') \bar{k}(s') \beta(s') ds' \quad (16)$$

$$\beta(s) = \frac{2\pi \bar{\gamma}(s)}{\delta(s)} \quad (17)$$

Within the CG approximation, the equivalent width is given in closed form by

$$\frac{\bar{W}(s)}{\delta} = \frac{\beta_e(s)}{\pi} I[\pi x(s)] \quad (18)$$

In the more sophisticated derivative approximation, <sup>(10)</sup>

$$y(s) = y[\pi x(s), \rho(s), q(s)] \quad (19)$$

where

$$y(\eta, \rho, q) = \frac{2}{\pi} \int_0^\infty \left[ \int_0^1 \exp \left\{ -\frac{2\eta u^q}{1 + \rho^2 z^2} \right\} du \right] \frac{dz}{1 + z^2} \quad (20)$$

A numerical procedure for computing this function is discussed in Ref. (10). Briefly, the procedure consists of rewriting  $y(\eta, \rho, q)$  in an alternate form

$$y(\eta, \rho, q) = \frac{1}{q} y(\eta, \rho, 1) + \frac{q-1}{q} \int_0^1 y(xz^q, \rho, 1) dz$$

that relates  $y(\eta, \rho, q)$  to its value at  $q = 1$ . The integral term is evaluated numerically by Gaussian quadrature, and the function  $y(\eta, \rho, 1)$  is approximated by

$$y(\eta, \rho, 1) = \frac{2\rho(1+\eta) + (1+\rho^2) \sqrt{1+2\eta}}{\sqrt{1+2\eta} [\rho + \sqrt{1+2\eta}]^2} \quad (21)$$

The addition parameter  $q(s)$  is defined as

$$q(s) = \frac{\bar{\delta}_e(s)}{\bar{\delta}(s)} \quad (22)$$

where

$$\bar{\delta}_e(s) = \frac{1}{u(s) \bar{k}_e(s)} \int_0^s c(s') p(s') \bar{k}(s') \bar{\delta}(s') ds' \quad (23)$$

In the derivative approximation,  $\bar{W}(s)/\delta$  must be computed according to Eq. (7).

The third model is a hybrid of a model developed in Ref. (9) that takes greater account of the differences in properties between the emission and absorption segments of the total optical path (but still treats the segments as coupled), and a model developed in Ref. (10) that treats all lines in  $\Delta\nu$  as though they vary with temperature in an identical manner. This hybrid model (2-path mean line approximation) is applied only for  $s_0 \leq s \leq s_m$  (see Figure 1). For  $s < s_0$ , the CG or derivative approximation is used. In this model

$$y(s) = y\left[\frac{\pi x_0}{q_0}, \frac{\pi x(s)}{q(s)}, \rho_0, \rho(s)\right] \quad (24)$$

where

$$y(\eta_1, \eta_2, \rho_1, \rho_2) = \begin{cases} \frac{1}{\rho_1^2 \rho_2^2} [A + B(p_1, p_2) + B(p_2, p_1)] & p_1 \neq p_2 \neq 1 \\ \frac{C(p_1)}{\rho_1^2 \rho_2^2} & p_1 \neq p_2 = 1 \\ \frac{C(p_2)}{\rho_1^2 \rho_2^2} & p_2 \neq p_1 = 1 \\ y(\eta_2, \rho_2) & p_1 = p_2 \text{ and } \eta_1 = 0 \\ y(\eta_1, \rho_1) & p_1 = p_2 \text{ and } \eta_2 = 0 \end{cases} \quad (25)$$

$$A = \frac{(1 - \rho_1^2)(1 - \rho_2^2)}{(1 - p_1)(1 - p_2)} \quad (26)$$

$$B(p, p') = \frac{(1 - \rho_1^2 p)(1 - \rho_2^2 p)}{(1 - p)(p' - p)\sqrt{p}} \quad (27)$$

$$C(p) = \frac{(1 - \rho_1^2 p)(1 - \rho_2^2 p)}{\sqrt{p}(1 - p)^2}$$

$$- \frac{1}{(1 - p)} \left[ \rho_1^2(1 - \rho_2^2) + \rho_2^2(1 - \rho_1^2) + \frac{(1 - \rho_1^2)(1 - \rho_2^2)(3 - p)}{2(1 - p)} \right] \quad (28)$$

$$y(\eta, \rho) = \frac{2\rho(1 + \eta) + (1 + \rho^2) \sqrt{1 + 2\eta}}{\sqrt{1 + 2\eta} [\rho + \sqrt{1 + 2\eta}]^2} \quad (29)$$

$$p_1 = \frac{1}{2} \left[ b + \sqrt{b^2 - 4c} \right] \quad (30)$$

$$p_2 = \frac{1}{2} \left[ b - \sqrt{b^2 - 4c} \right] \quad (31)$$

$$b = \frac{1 + 2\eta_1}{\rho_1^2} + \frac{1 + 2\eta_2}{\rho_2^2} \quad (32)$$

$$c = \frac{1 + 2(\eta_1 + \eta_2)}{\rho_1^2 \rho_2^2} \quad (33)$$

The  $x$ ,  $\rho$  and  $q$  parameters in Eq. (24) are obtained from Eqs. (12) through (17) and Eqs. (22) and (23) with the following modifications: (1) for subscript zero parameters, the lower and upper integration limits are 0 and  $s_0$ , respectively; (2) for nonsubscripted parameters, the limits are  $s_0$  and  $s$ , respectively.

#### D. y-Functions for Doppler Line Shape

In the CG approximation

$$y(s) = y[\pi x(s), \rho(s)] \quad (34)$$

where

$$y(\eta, \rho) = (2 - \rho) \frac{dH(\eta)}{d\eta} + (\rho - 1) \frac{H(\eta)}{\eta} \quad (35)$$

and

$$H(\eta) = \frac{2}{\sqrt{\pi}} \int_0^{\infty} \ln \left[ 1 + \eta e^{-u^2} \right] du \quad (36)$$

The functions  $H(\eta)$  and  $dH(\eta)/d\eta$  can be obtained by interpolation on the data of Table 3. For small  $\eta$

$$H(\eta) \approx - \sum_{n=0}^{\infty} \frac{(-\eta)^{n+1}}{(n+1)^{3/2}} \quad (37)$$

$$\frac{dH(\eta)}{d\eta} \approx \sum_{n=0}^{\infty} \frac{(-\eta)^n}{\sqrt{n+1}} \quad (38)$$

while for large  $\eta$

$$H(\eta) \approx \frac{4}{3\sqrt{\pi}} (\ln \eta)^{3/2} \left[ 1 + \frac{\pi^2/8}{(\ln \eta)^2} + \frac{7\pi^4/640}{(\ln \eta)^4} + \dots \right] \quad (39)$$

$$\frac{dH(\eta)}{d\eta} \approx \frac{2}{\eta \sqrt{\pi}} \sqrt{\ln \eta} \left[ 1 - \frac{\pi^2/24}{(\ln \eta)^2} - \frac{35\pi^4/1920}{(\ln \eta)^4} + \dots \right] \quad (40)$$

The arguments  $x(s)$  and  $\rho(s)$  are defined as for the Lorentz line shape by Eqs. (12) through (16), but with  $\beta(s)$  defined as

$$\beta(s) = \sqrt{\frac{\pi}{\ln 2}} \frac{\gamma(s)}{\delta(s)} \quad (41)$$

where  $\gamma(s)$  is the Doppler line width

Table 3. Curve of Growth Functions for Statistical  
Doppler Line Band Model

$\eta$	$H(\eta)$	$dH(\eta)/d\eta$
0.1	0.09665	0.93460
0.2	0.18722	0.87828
0.4	0.35325	0.78593
0.6	0.50289	0.71310
0.8	0.63940	0.65398
1.0	0.76515	0.60490
2.0	1.28138	0.44564
4.0	2.00567	0.29978
6.0	2.52794	0.22935
8.0	2.94136	0.18717
10	3.28568	0.15883
20	4.47964	0.092598
40	5.84661	0.052199
60	6.71916	0.036911
80	7.36866	0.028752
100	7.88910	0.023642
200	9.59377	0.012759
400	11.4233	0.006813
600	12.5478	0.004702
800	13.3689	0.003609
1000	14.0187	0.002937



$$\gamma(s) = 3.56817 \times 10^{-7} \nu \sqrt{\frac{T(s)}{m}} \quad (42)$$

( $\nu$  has unit  $\text{cm}^{-1}$ ,  $T(s)$  has unit  $^{\circ}\text{K}$  and  $m$  is the atomic mass number of the molecular species.) Note that  $\beta(s)$  for the Doppler model is defined in terms of the parameter  $\bar{\delta}(s)$  appropriate for the Lorentz model. This is a necessary approximation since an adequate definition for the mean line spacing parameter in the Doppler statistical model does not exist.

The equivalent width within the CG approximation for the Doppler line shape is

$$\frac{\bar{W}(s)}{\bar{\delta}} = \frac{\beta_e(s)}{\pi} H[\pi x(s)] \quad (43)$$

The Doppler equivalent of the Lorentz derivative approximation [Eq. (19)], is not convenient for practical application. A related model based on the mean-line approximation discussed above is used in this case. The  $y$ -function is

$$y(s) = y\left[\frac{\pi x(s)}{q(s)}, \rho'(s)\right] \quad (44)$$

where

$$y(\eta, \rho) = \frac{2}{\sqrt{\pi}} \int_0^{\infty} \frac{\exp(-z^2)}{[1 + \eta \exp(-\rho^2 z^2)]} dz \quad (45)$$

For small  $\eta$ ,  $y(\eta, \rho)$  can be computed from

$$y(\eta, \rho) \approx \sum_{n=0}^{\infty} \frac{(-\eta)^n}{\sqrt{1 + n \rho^2}} \quad (46)$$

whereas for  $\rho \lesssim 0.5$ , the approximation

$$y(\eta, \rho) \approx \frac{1}{\sqrt{(1 + \eta) [1 - \eta (\rho^2 - 1)]}} \quad (47)$$

is accurate to better than one percent. For other  $(\eta, \rho)$  conditions,  $y(\eta, \rho)$  can be obtained for most practical applications by interpolation on the data of Table 4.

Similarly, the Doppler equivalent of the 2-path mean line approximation [Eq. (24)], for Lorentz lines is not practical. The following 2-path approximation is based on a rational approximation of the Doppler line shape by a parabolic line shape [see Ref. (9)]. The  $y$ -function is

$$y(s) = y \left[ \frac{\pi x_0}{q_0}, \frac{\pi x(s)}{q(s)}, \rho_0, \rho(s) \right] \quad (48)$$

where

$$y(\eta_1, \eta_2, \rho_1, \rho_2) = \begin{cases} g(\eta_1, \eta_2, \rho_1, \rho_2, 0, 1) & \rho_2 \leq \rho_1 \leq 1 \\ g(\eta_1, \eta_2, \rho_1, \rho_2, 0, 1/\rho_1) + g(0, \eta_2, \rho_1, \rho_2, 1/\rho_1, 1) & \rho_2 \leq 1 \leq \rho_1 \\ g(\eta_1, \eta_2, \rho_1, \rho_2, 0, 1/\rho_1) + g(0, \eta_2, \rho_1, \rho_2, 1/\rho_1, 1/\rho_2) + g_0(\rho_2) & 1 \leq \rho_2 \leq \rho_1 \\ g(\eta_1, \eta_2, \rho_1, \rho_2, 0, 1) & \rho_1 \leq \rho_2 \leq 1 \\ g(\eta_1, \eta_2, \rho_1, \rho_2, 0, 1/\rho_2) + g(\eta_1, 0, \rho_1, \rho_2, 1/\rho_2, 1) & \rho_1 \leq 1 \leq \rho_2 \\ g(\eta_1, \eta_2, \rho_1, \rho_2, 0, 1/\rho_2) + g(\eta_1, 0, \rho_1, \rho_2, 1/\rho_2, 1/\rho_1) + g_0(\rho_1) & 1 \leq \rho_1 \leq \rho_2 \end{cases} \quad (49)$$

Table 4. Equivalent Width Derivation Function for Statistical Doppler Line Band Model

$\eta$	$\rho$						
	5.00E-1	1.00E+0	1.25E+0	1.50E+0	2.00E+0	3.00E+0	5.00E+0
1.0E-2	0.99114E+0	0.99299E+0	0.99380E+0	0.99450E+0	0.99556E-0	0.99686E-0	0.99805E-0
2.0E-2	0.98243E+0	0.98608E+0	0.98770E+0	0.98907E+0	0.99119E-0	0.99377E-0	0.99613E-0
5.0E-2	0.95723E+0	0.96603E+0	0.96995E+0	0.97329E+0	0.97844E-0	0.98474E-0	0.99053E-0
1.0E-1	0.91803E+0	0.93460E+0	0.94207E+0	0.94846E+0	0.95836E-0	0.97050E-0	0.98168E-0
2.0E-1	0.84868E+0	0.87828E+0	0.89190E+0	0.90367E+0	0.92200E-0	0.94464E-0	0.96560E-0
5.0E-1	0.69248E+0	0.74750E+0	0.77433E+0	0.79799E+0	0.83553E-0	0.88273E-0	0.92692E-0
1.0E+0	0.53069E+0	0.60490E+0	0.64392E+0	0.67937E+0	0.73706E-0	0.81132E-0	0.88198E-0
2.0E+0	0.36239E+0	0.44564E+0	0.49455E+0	0.54100E+0	0.61957E-0	0.72444E-0	0.82669E-0
5.0E+0	0.18622E+0	0.25945E+0	0.31182E+0	0.36593E+0	0.46452E-0	0.60548E-0	0.74932E-0
1.0E+1	0.10301E+0	0.15883E+0	0.20643E+0	0.25986E+0	0.36450E-0	0.52442E-0	0.69490E-0
2.0E+1	0.54426E-1	0.92598E-1	0.13195E+0	0.18053E+0	0.28411E-0	0.45506E-0	0.64664E-0
5.0E+1	0.22544E-1	0.43173E-1	0.70728E-1	0.10995E+0	0.20490E-0	0.38046E-0	0.59211E-0
1.0E+2	0.11408E-1	0.23642E-1	0.43542E-1	0.75384E-1	0.16102E-0	0.33469E-0	0.55672E-0
2.0E+2	0.57384E-2	0.12759E-1	0.26649E-1	0.51787E-1	0.12735E-0	0.29611E-0	0.52535E-0
5.0E+2	0.23038E-2	0.55566E-2	0.13871E-1	0.31709E-1	0.94277E-1	0.25368E-0	0.48873E-0
1.0E+3	0.11533E-2	0.29368E-2	0.84594E-2	0.21992E-1	0.75569E-1	0.22668E-0	0.46396E-0
2.0E+3	0.57700E-3	0.15432E-2	0.51628E-2	0.15322E-1	0.60853E-1	0.20319E-0	0.44126E-0
5.0E+3	0.23088E-3	0.65458E-3	0.26937E-2	0.95640E-2	0.45971E-1	0.17650E-0	0.41390E-0
1.0E+4	0.11546E-3	0.34067E-3	0.16503E-2	0.67263E-2	0.37322E-1	0.15906E-0	0.39491E-0
2.0E+4	0.57731E-4	0.17676E-3	0.10132E-2	0.47468E-2	0.30380E-1	0.14358E-0	0.37718E-0
5.0E+4	0.23093E-4	0.73960E-4	0.53344E-3	0.30083E-2	0.23224E-1	0.12570E-0	0.35546E-0
1.0E+5	0.11547E-4	0.38163E-4	0.32916E-3	0.21370E-2	0.18996E-1	0.11383E-0	0.34018E-0

$$g(\tau_1, \tau_2, \rho_1, \rho_2, a, b) = \frac{3}{2} \left[ \frac{b-a}{x} + \frac{(x-\alpha)}{2x\sqrt{\alpha x}} \ln \left\{ \frac{\alpha+b\sqrt{\alpha x}}{\alpha-b\sqrt{\alpha x}} \frac{\alpha-a\sqrt{\alpha x}}{\alpha+a\sqrt{\alpha x}} \right\} \right] \quad (50)$$

$$g_0(\rho) = \frac{\rho-1}{2\rho^3} (\rho^2 - 2\rho - 2) \quad (51)$$

$$\alpha = 1 + \tau_1 + \tau_2 \quad (52)$$

$$x = x_1 \rho_1^2 + x_2 \rho_2^2 \quad (53)$$

The  $x$ ,  $\rho$ , and  $q$  arguments of Eq. (48) are computed with the same integration limit modifications as are used in the Lorentz 2-path model.  $\beta(s)$  is computed from Eqs. (41) and (42).

#### E. y-Function for Voigt Line Shape

The band model formulation for Voigt line shape is based on an approximation devised by Rodgers and Williams<sup>(11)</sup> for isolated lines and uniform optical paths. The equivalent width and y-function are computed assuming first a pure Lorentz line shape and second a pure Doppler (or parabolic) line shape according to the methods of the preceding paragraphs. The equivalent width for the Voigt line is then approximated as

$$\frac{\bar{W}(s)}{\delta} = \sqrt{\left[ \frac{\bar{W}_L(s)}{\delta} \right]^2 + \left[ \frac{\bar{W}_D(s)}{\delta} \right]^2 - \left[ \frac{\bar{W}_L(s)}{\delta} \frac{\bar{W}_D(s)}{\delta} / \frac{\bar{W}_W(s)}{\delta} \right]^2} \quad (54)$$

where

$$\frac{\bar{W}_W(s)}{\delta} = u(s) \bar{k}_e(s) \quad (55)$$

in the single-path models and

$$\frac{\overline{W}_W(s)}{\delta} = u_0 \overline{k}_0 + u(s) \overline{k}_e(s) \quad (56)$$

in the 2-path models for  $s > s_0$ .

The derivative function is given by

$$y(s) = A(s) y_L(s) + B(s) y_D(s) + C(s) \quad (57)$$

where

$$A(s) = \frac{\overline{W}_L(s)/\delta}{\overline{W}(s)/\delta} \left\{ 1 - \left( \frac{\overline{W}_D(s)/\delta}{\overline{W}_W(s)/\delta} \right)^2 \right\} \quad (58)$$

$$B(s) = \frac{\overline{W}_D(s)/\delta}{\overline{W}(s)/\delta} \left\{ 1 - \left( \frac{\overline{W}_L(s)/\delta}{\overline{W}_W(s)/\delta} \right)^2 \right\} \quad (59)$$

$$C(s) = \frac{\overline{W}_W(s)/\delta}{\overline{W}(s)/\delta} \left( \frac{\overline{W}_L(s)/\delta}{\overline{W}_W(s)/\delta} \right)^2 \left( \frac{\overline{W}_D(s)/\delta}{\overline{W}_W(s)/\delta} \right)^2 \quad (60)$$

### III. COMPUTER CODE ATLES

#### A. Flow Diagram

The main code ATLES and its associated subprograms are coded in FORTRAN IV compatible with The Aerospace Corporation CDC 7600 computer and SCOPE operating system. A simplified flow diagram for ATLES is shown in Figure 2. This section gives a brief discussion of each of the numbered blocks on the flow chart. Sections B through E give more detailed information on critical computation routines.

1. Each run of the program requires the input of various numerical data and control data to specify the operating mode of the program. The preparation of input data is detailed in Section IV. The read-in of all data for a computational run is effected by a call-to-subroutine INPUT. This subroutine either reads data directly from the card deck input stream or calls other subroutines that read data from the input stream or from attached tape or disc input devices. Subroutines that may be called by INPUT and their function are:

MODATM	Read altitude profiles of a model atmosphere.
BAND	Read band model parameters for a single species.
PLUME	Read pTc data for an exhaust plume.
PDATA	Read pTc data for a single line of sight through an absorption or emission cell.
SGRID	Read plume projected area integration coordinates.

Data read directly by INPUT include:

- a. Control data specifying: (1) Whether calculations are to be made on an isolated absorption path, an isolated emission path or a coupled absorption-emission path; (2) Whether the absorption path is an atmospheric slant path or an absorption cell path; and (3) Whether the radiation source is a plume or an emission cell path.

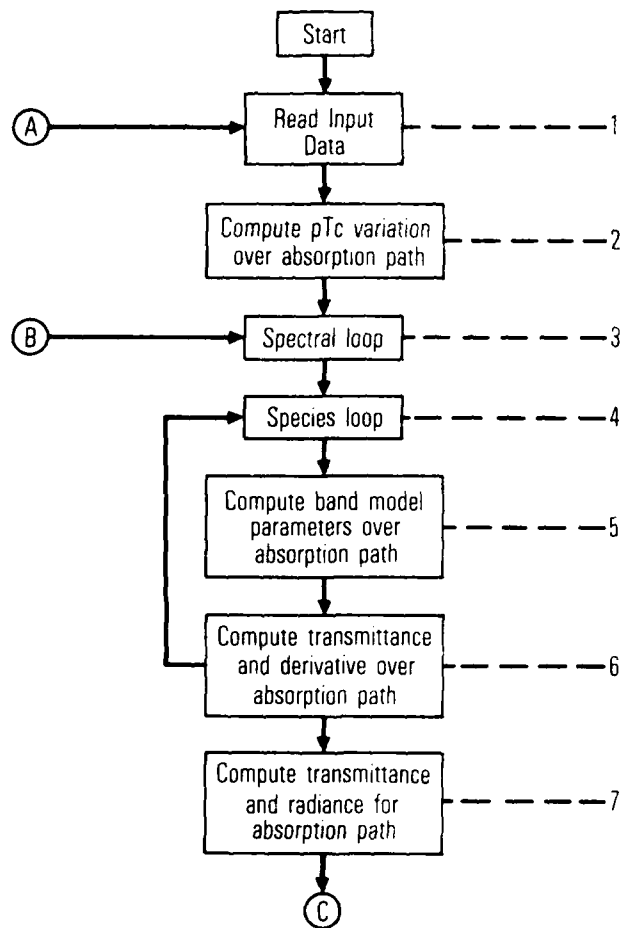


Figure 2. ATLES Flow Diagram

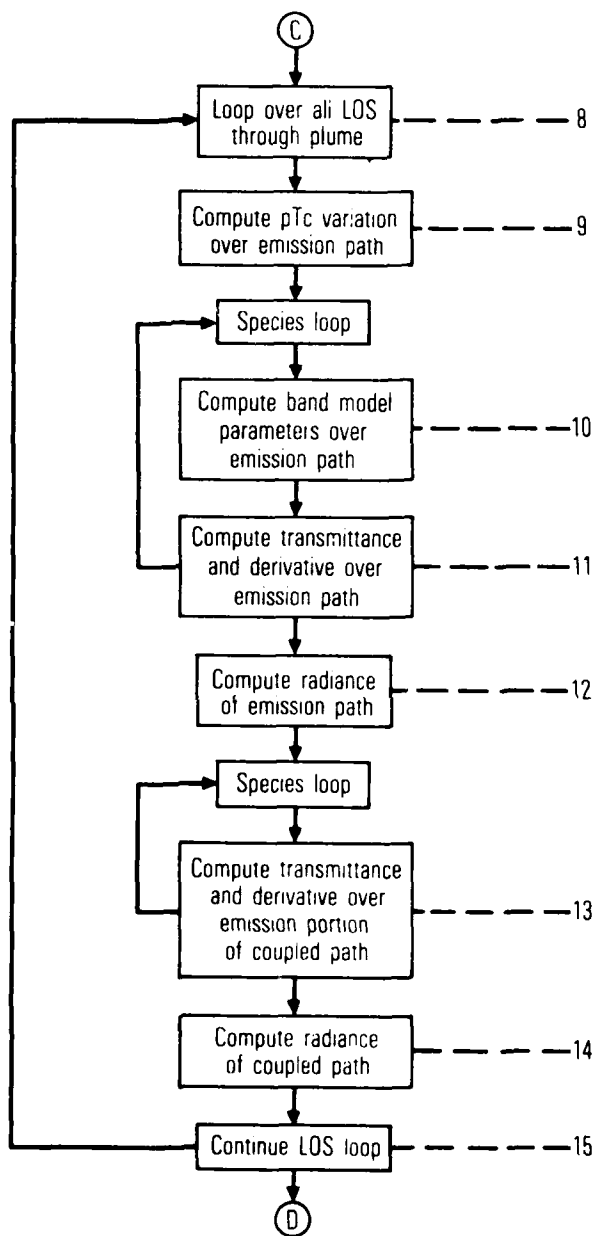


Figure 2. ATLES Flow Diagram (Continued)



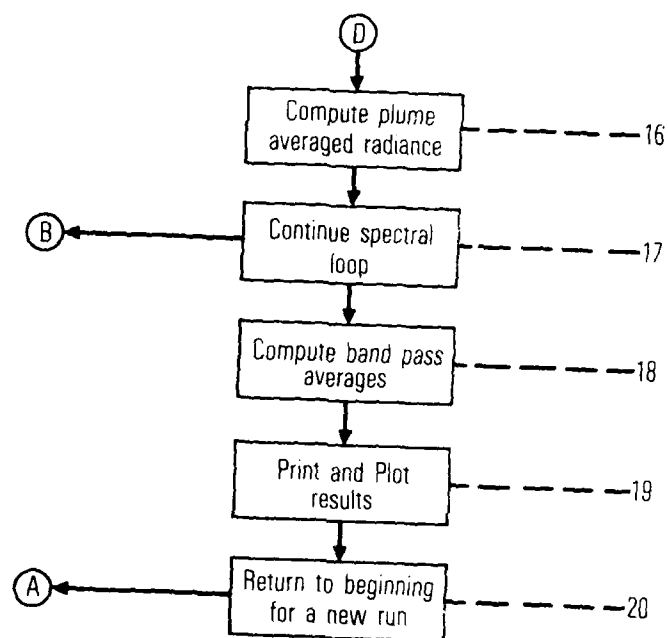


Figure 2. ATLES Flow Diagram (Continued)

- b. Spectral data defining: (1) The spectral region over which calculations will be made and the step size; (2) The spectral unit; and (3) Bandpasses over which computed spectral data will be averaged.
- c. Band model data specifying the lineshape and inhomogeneity modes to be used.
- d. Integration step size data for path integrations over the absorption and emission portions of the optical line of sight and for area integration over the projected area of a plume. The latter data consist of grid coordinates defining many lines of sight through the plume.
- e. Information specifying those species to be included in the absorption path and those to be included in the emission path.
- f. Geometry data defining the atmospheric slant path and plume aspect angle.

2.\* If absorption over an atmospheric slant path is to be computed, calls to the subroutines VIEW and APATH are made. The former computes the altitude variation over the slant path as a function of distance along the path, and the second interpolates for pTc data along the path using the altitude variation determined by VIEW and the model atmosphere read in by MODATM. The number of points along the slant path and the geometry of the slant path are defined as part of the input (step 1). If an absorption cell is being considered, the pTc data along the path are computed in subroutine LPATH by linear interpolation on data read in by PDATA.

---

\*More detailed information on subroutines MODATM and VIEW is given in Sections B and C, respectively.

3. A spectral loop over limits and increment defined as part of the primary input is now initiated. If the problem consists of computing source radiation only, a skip to step 8 occurs now.
4. Band model calculations are performed for one species at a time. This step initiates a loop over all species specified by the primary input data to be in the atmosphere (or absorption cell).
5. Subroutine BPARAM is used to compute band model parameters along the absorption path with the data read in by BAND and the pTc variation determined in step 2. Linear interpolation on both  $\nu$  and T is employed except for T outside the range of the input band model parameters table. Semilogarithmic extrapolation is used in this case.
- 6.\* Subroutine DELTRAN is the core of the band modeling routines. With the pTc and band model parameters determined in steps 2 and 5, respectively, the transmittance and transmittance derivative along the optical path are computed according to the models of Section II. Subroutines that may be called by DELTRAN, their purpose, and the method of computation are:
 

FI	Compute equivalent width function for a band of Lorentz lines (analytic function).
GI	Compute equivalent width function for a band of Doppler lines (asymptotic series and quadratic, semilog interpolation).
WMIX	Compute equivalent width for a band of Voigt lines according to the approximation of Rodgers and Williams (analytic function).

---

\*More detailed information on subroutine DELTRAN is given in Section E.

YCGL Compute equivalent width derivative function for a band of Lorentz lines in the Curtis-Godson approximation (analytic function).

YDRL Compute equivalent width derivative function for a band of Lorentz lines in the derivative approximation. This subfunction uses the subprogram YLSL which computes the derivative function in the Lindquist-Simmons approximation (numerical integration by Gaussian quadrature).

Y2MLL Compute equivalent width derivative function for a band of Lorentz lines in the 2-path, mean-line approximation (analytic functions). YLSL is used by this subfunction also.

YCGD Compute equivalent width derivative function for a band of Doppler lines in the Curtis-Godson approximation (asymptotic series and parabolic, semi-logarithmic interpolation).

YMLD Compute equivalent width derivative function for a band of Doppler lines in the mean-line approximation (series solution, analytic approximation and tabular interpolation).

Y2MLP Compute equivalent width derivative function for a band of Doppler lines (parabolic approximation) in the 2-path, mean-line approximation. The subfunction FUNC is called by Y2MLP (analytic functions).

YMX Compute equivalent width derivative function for a band of Voigt lines using the approximation of Rodgers and Williams (analytic functions).

7. When the transmittance and derivative for each species in the absorption path has been determined, the total transmittance and radiance of the path is computed by subroutine RADNCE. The path integration is handled by trapezoidal quadrature.

8. If the radiation source is a plume, a two-dimensional loop over the projected plume area is now initiated using the coordinate data read in by SGRID. If the source is an emission cell, the loop is gone through just once. If only an absorption path is being considered, no loop is made, and an immediate continuation of the spectral loop takes place.
- 9.\* If the source is a plume, subroutine SPATH is used to compute the pTc variation over the portion of the line of sight within the plume (the emission path). The plume data read in by PLUME is used for this purpose. If the source is an emission cell, the pTc variation is computed by subroutine LPATH and data read in by PDATA.
- 10-12. Steps 10 through 12 are similar to steps 4 through 7 except that the total radiance for the emission source is computed. These steps compute the source radiance for no attenuation by the absorption path.
- 13-14. Again, these steps are similar to steps 10 through 12 except that now atmospheric attenuation is included. If only an emission path is being considered, this step is bypassed. Note that the band model parameters over the emission path do not have to be computed in this routine since they have already been computed in step 10.
15. Continue loop over all lines of sight through plume.
16. When the radiance of all lines of sight through the plume has been determined, spatial integrations over the plume are performed in subroutine PLUMAVE. Trapezoidal quadrature in both plume directions are used for these integrations.
17. Continue spectral loop.

---

\*More detailed information on subroutine SPATH is given in Section D.

18. At the completion of step 17, the spatial and spectral variation of both the unattenuated and attenuated plume radiance has been determined, and the average spectra of these two radiances over the projected area of the plume has been computed. Subroutine BNDPASS is now called to compute bandpass averages of the average radiance spectra and of atmospheric transmittance spectra. Linear interpolation and trapezoidal quadrature are employed in this routine.
19. Computed results are now listed by subroutine OUTPUT and (optionally) plotted by subroutine SPLOT. The nominal listing consists of a summary listing of input data; the spectra for (1) Atmospheric or absorption path radiance; (2) Unattenuated source radiance averaged over plume; (3) Attenuated source radiance averaged over plume; (4) Atmospheric or absorption path transmittance; (5) Effective atmospheric or absorption path transmittance; and bandpass averages for each of these five spectra. An optional listing of the spatial variation of bandpass averaged radiances over the projected area of a plume is made by subroutine MAP.
20. Return to beginning of program for a new computational run.

#### B. Subroutine MODATM

This subroutine is designed around the model atmosphere profiles of McClatchey, et al. <sup>(2)</sup> Data defining the pressure, temperature and water concentration at the specific altitudes 0, 1, 2, 3, ..., 24, 25, 30, 35, ..., 50, 70 and 100km are read in. The input data deck structure is given in Figure 13. The pressure and water concentration data may be entered in natural units of atm and mole fraction, respectively, or in the McClatchey, et al., units of mb and g/m<sup>3</sup>, respectively. If the latter, conversion to natural units is made by

$$p(\text{atm}) = \frac{p(\text{mb})}{1.013 \times 10^3}$$

and

$$c_{\text{H}_2\text{O}} \text{ (mole fraction)} = 4.559 \times 10^{-6} \frac{\rho_{\text{H}_2\text{O}} \text{ (g/m}^3\text{)} T(^{\circ}\text{K})}{p(\text{atm})}$$

Data entered at the altitudes specified above are used to construct an altitude interpolation table with the pTc data given at each 1-km step between 0 and 100km. Linear interpolation on T, log(p) and log( $c_{\text{H}_2\text{O}}$ ) for  $20 \leq z \leq 50$  and quadratic interpolation on these same quantities for  $50 \leq z \leq 100$  are used to construct the table.

#### C. Subroutine VIEW

Subroutine VIEW accepts data defining the geometry configuration of a sensor and target and computes the altitude variation along the slant path between these two positions. Two geometry cases are considered. The first consists of a sensor above the atmosphere and a target within the atmosphere. The data entered for this case are the target altitude h, the target-to-sensor zenith angle  $\theta$ , and an altitude  $z_m$  defining the top of the atmosphere. The slant path defined by these variables is shown in Figure 3. The path position  $s = 0$  is defined as the point where the line of sight from the sensor to the target enters the atmosphere. The total path length in the atmosphere is

$$s_m = - (R_e + h) \cos \theta + \sqrt{(R_e + z_m)^2 - (R_e + h)^2 \sin^2 \theta}$$

where  $R_e$  is the radius of the earth. The value  $R_e = 6368\text{km}$  is used. For this geometry, and for any value of  $0 \leq s \leq s_m$ , the altitude at s is computed from

$$z(s) = \sqrt{(R_e + z_m)^2 + s^2 - 2s [s_m + (R_e + h) \cos \theta]} - R_e$$

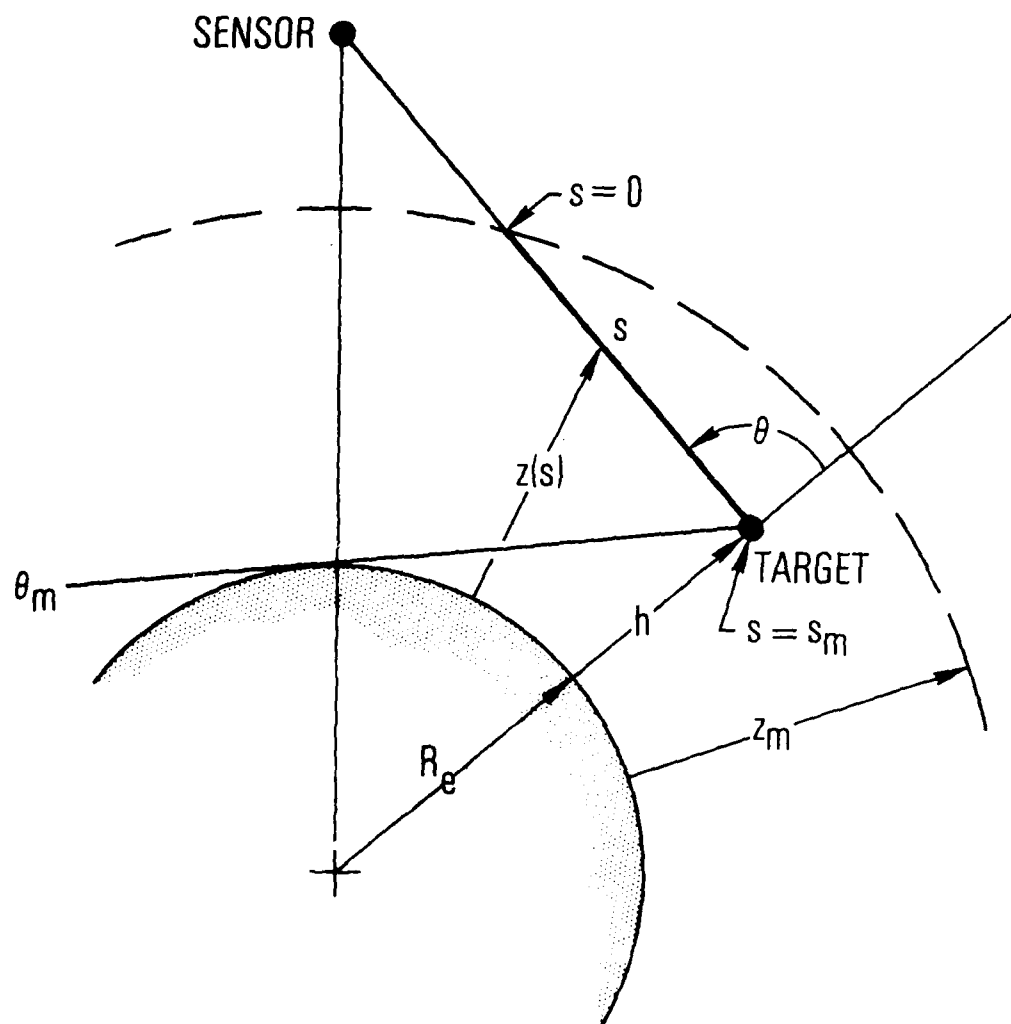


Figure 3. Atmospheric Slant Path Geometry for a Sensor above the Atmosphere



The maximum zenith angle allowed for this case is

$$\theta_m = \pi - \sin^{-1} \left( \frac{R_e}{R_e + h} \right)$$

Nominally,  $z_m = 100\text{km}$  is used. For  $h = z_m$  then, the maximum allowed zenith angle is  $\sim 100^\circ$ .

The second viewing geometry case consists of a sensor within the atmosphere and a target either within or outside the atmosphere. The data entered for this case are the sensor altitude  $H$ , the sensor-to-target zenith angle  $\varphi$ , the range from the sensor to target  $r$ , and again  $z_m$ . The slant path for this case and with the target within the atmosphere is shown in Figure 4. The target altitude is computed by

$$h = \sqrt{(R_e + H)^2 + r^2 + 2(R_e + h) r \cos \varphi} - R_e$$

The total path length in the atmosphere is computed from

$$s_m = \begin{cases} r & h \leq z_m \\ - (R_e + H) \cos \varphi + \sqrt{(R_e + z_m)^2 - (R_e + H)^2 \sin^2 \varphi} & h > z_m \end{cases}$$

and the altitude variation along the path for  $0 \leq s \leq s_m$  by

$$z(s) = \sqrt{(R_e + H)^2 + s^2 - 2s(R_e + H) \cos \varphi} - R_e$$

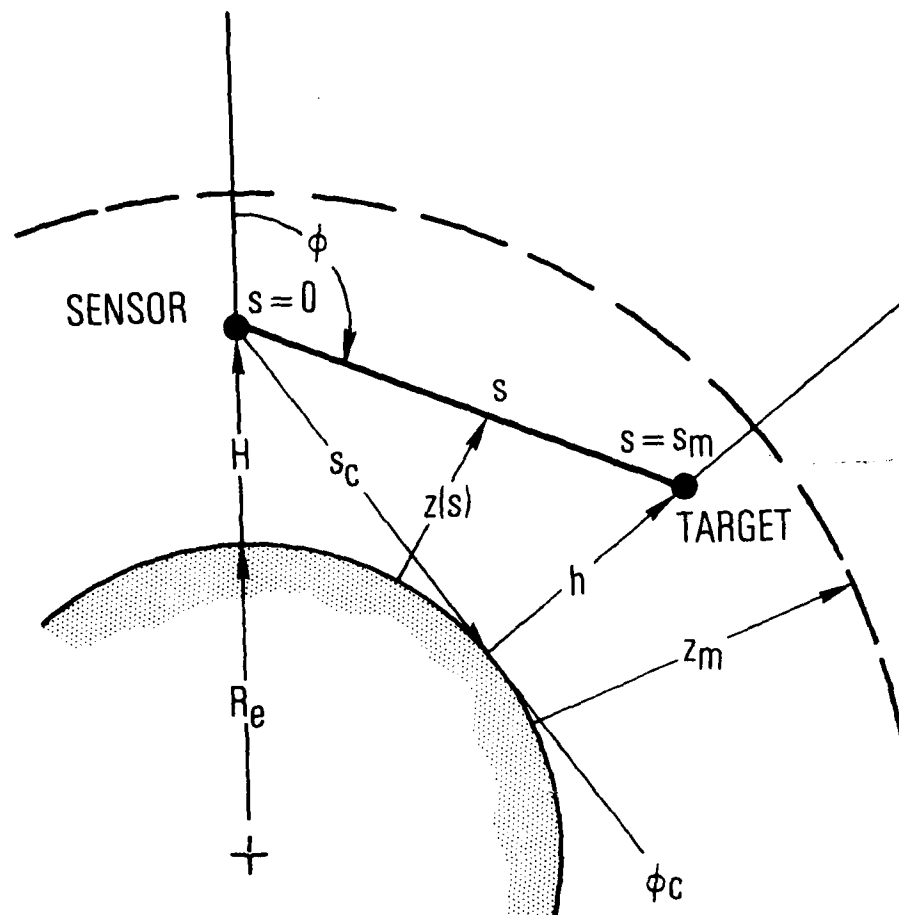


Figure 4. Atmospheric Slant Path Geometry for a Sensor within the Atmosphere

If the zenith angle is greater than the critical angle

$$\varphi_c = \pi - \sin^{-1} \left( \frac{R_e}{R_e + H} \right),$$

the line-of-sight from the sensor intersects the earth. In this case, the range  $r$  must be less than the critical length

$$s_c = - (R_e + H) \cos \varphi - \sqrt{R_e^2 - (R_e + H)^2 \sin^2 \varphi}$$

Neither of the geometry cases consider line of sight curvature due to refraction.

The optical path within the atmosphere is divided into  $N$  intervals ( $N$  is an input parameter to the subroutine), and the altitudes at the  $N + 1$  points between  $s = 0$  and  $s = s_m$  computed according to the previous equations. The division is made so that each interval contains approximately the same mass. This is accomplished by assuming an isothermal, exponential pressure atmosphere, which gives the algorithm

$$s_2 = - \frac{\beta}{\cos \alpha} \ln \left\{ e^{-(s_1/\beta) \cos \alpha} - \frac{1}{N} \left[ 1 - e^{-(s_m/\beta) \cos \alpha} \right] \right\}$$

Given the path position  $s_1$ ,  $s_2 > s_1$  is the path position such that  $1/N$  of the integrated mass along the path lies between  $s_1$  and  $s_2$ . A starting value of  $s_1 = 0$  is used. The computed value of  $s_2$  becomes the next value of  $s_1$ , etc. The process is repeated  $N$  times.  $\beta$  is the exponential scale height of the atmosphere. The value  $\beta = 7.32\text{km}$  is used. For the geometry case of a sensor within the atmosphere,  $\alpha = \varphi$ . For the exoatmospheric sensor case,  $\alpha = \pi - \theta$ . For  $\alpha$  within  $2^\circ$  of  $90^\circ$  (nearly horizontal paths), a simple equal-interval division of the path is made.

The final results of the subroutine are the two arrays  $s(i)$ ,  $z(i)$ ,  $i = 1, N + 1$ . These arrays, along with the 1-km interval atmosphere profile table computed in subroutine MODATM are passed to subroutine APATH where an interpolation calculation is used to obtain pTc data at the  $N + 1$  points along the atmospheric slant path.

#### D. Subroutine SPATH

Subroutine SPATH computes the geometry of intersection (Figure 5) between a line of sight and a paraboloid plume control surface and interpolates for pTc data along the intersection chord. The plume geometry data  $R_o$  (nozzle exit radius),  $L$  (plume length), and  $R_m$  (maximum plume radius) are entered as input data through subroutine PLUME. Subroutine PLUME also enters the pTc data defining the plume within the paraboloid plume control surface (see Figure 14 for preparation of plume data). The line of sight through the plume is defined by three parameters:  $z_o$  is the axial distance at which the line of sight intersects the y-z plane (see Figure 5);  $d$  is the transverse distance from the x-z plane where the line of sight enters and exits the plume control surface; and  $\alpha$  is the aspect angle of the line of sight with the plume axis ( $0 \leq \alpha \leq 180^\circ$ ).

The values of  $R_o$ ,  $R_m$ ,  $L$ ,  $z_o$ ,  $d$ , and  $\alpha$  determine one of five basic intersection geometries that depend principally on which of the three surfaces (nozzle exit plane, paraboloid surface, end plane) the line of sight enters and exits the plume. These cases are illustrated in Figure 6. The case where the line of sight cannot enter the plume because of missile obscuration, or where the line of sight does not intersect the plume are handled as a sixth case by setting an obscuration flag. The cases for  $\alpha = 0$  and  $\alpha = \pi$  are also handled separately from the five basic intersection geometries.

The intersection cases are determined by comparisons with the four test quantities

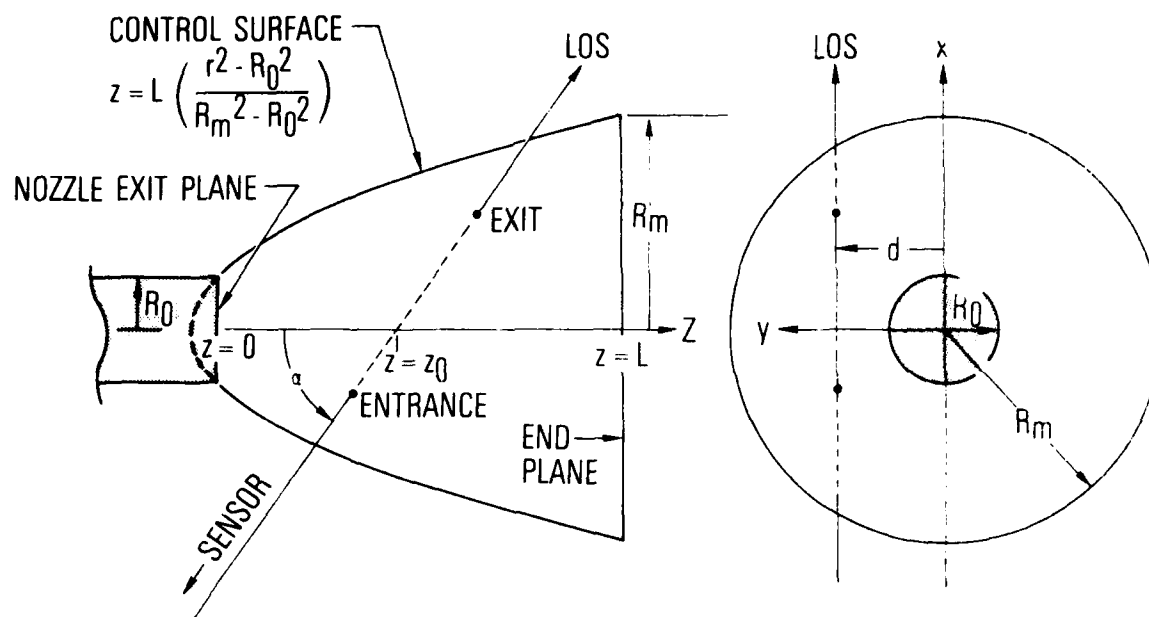


Figure 5. Geometry of Intersection between an Optical Line of Sight and Paraboloid Plume Control Surface

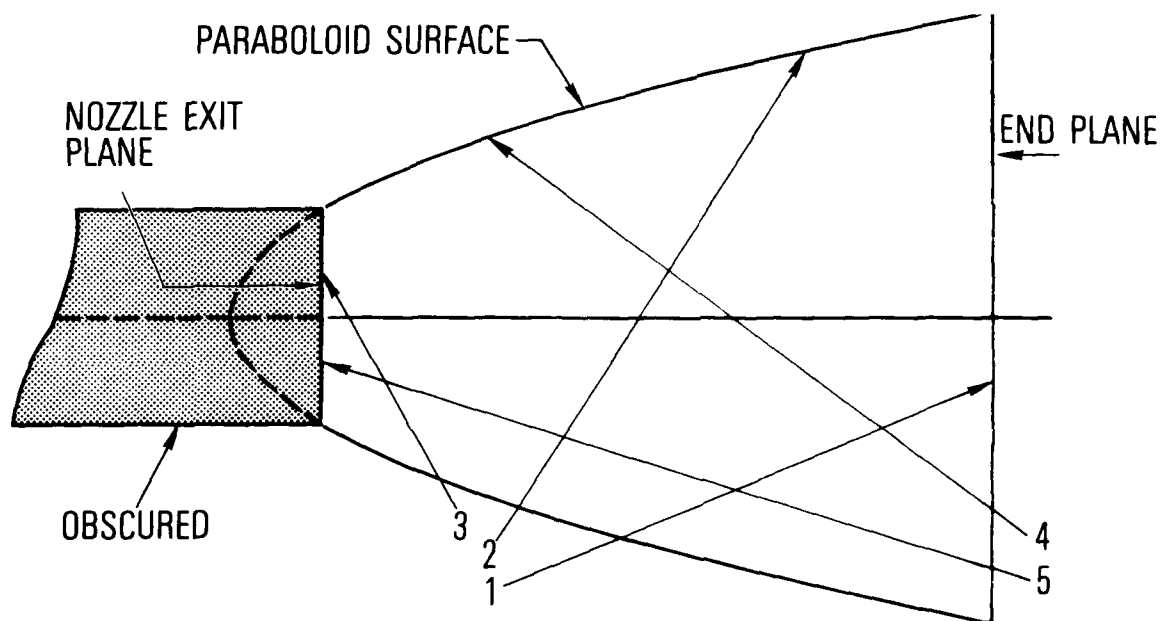


Figure 6. General Intersection Cases. NOTES:  
 (1) Cases 2 and 4 handle the case where, for  $\alpha \approx \pi/2$ , the LOS exits from the control surface on the same side that it enters. (2) Cases 3 and 5 can occur only for  $\alpha > \pi/2$  and  $d < R_0$ . If  $d > R_0$ , the LOS continue to the control surface and are handled by cases 2 and 4, respectively.

$$z_{\min} = \frac{L(d^2 - R_o^2)}{(R_m^2 - R_o^2)} - \frac{R_m^2 - R_o^2}{4L} \cot^2 \alpha$$

$$z_1 = L - \sqrt{R_m^2 - d^2} \cot \alpha$$

$$z_2 = L + \sqrt{R_m^2 - d^2} \cot \alpha$$

$$z_3 = \sqrt{R_o^2 - d^2} \cot \alpha$$

The significance of these quantities can be deduced from Figure 7. If  $z_o < z_{\min}$  or  $z_o > z_1$  ( $\alpha < \pi/2$ ) or  $z_o > z_2$  ( $\alpha > \pi/2$ ), the LOS misses the plume. Likewise, if  $d > R_m$ , the LOS misses the plume. The test parameter  $z_3$  is relevant only if  $d < R_o$  and is used to test for obscuration ( $\alpha < \pi/2$ ) or for cases where the LOS ends on the nozzle-plane. The LOS is obscured if: (1)  $\alpha < \pi/2$  and  $d < R_o$  and  $-z_3 < z_o < z_3$ ; or (2) If  $d < R_o$  when  $\alpha = 0$ . The test parameters  $z_1$  and  $z_2$  are used to differentiate between LOS that exit ( $\alpha < \pi/2$ ) on the control surface or end-plane and LOS that enter ( $\alpha > \pi/2$ ) on the control surface or end plane. The conditions that determine the various intersection cases are listed in Table 5. When the intersection case has been determined, the coordinates of the entrance ( $X_1, Z_1$ ) and exit ( $X_2, Z_2$ ) points between the LOS and the plume are computed. The appropriate assignments are indicated in Table 5. The various coordinate definitions are:

$$\left. \begin{aligned} x_{\pm} &= \frac{R_m^2 - R_o^2}{2L} \cot \alpha \pm \sqrt{\frac{R_m^2 - R_o^2}{L}} (z_{\min} - z_o) \\ z_{\pm} &= z_o + x_{\pm} \cot \alpha \end{aligned} \right\} \begin{array}{l} \text{entrance or exit} \\ \text{on control surface} \end{array}$$

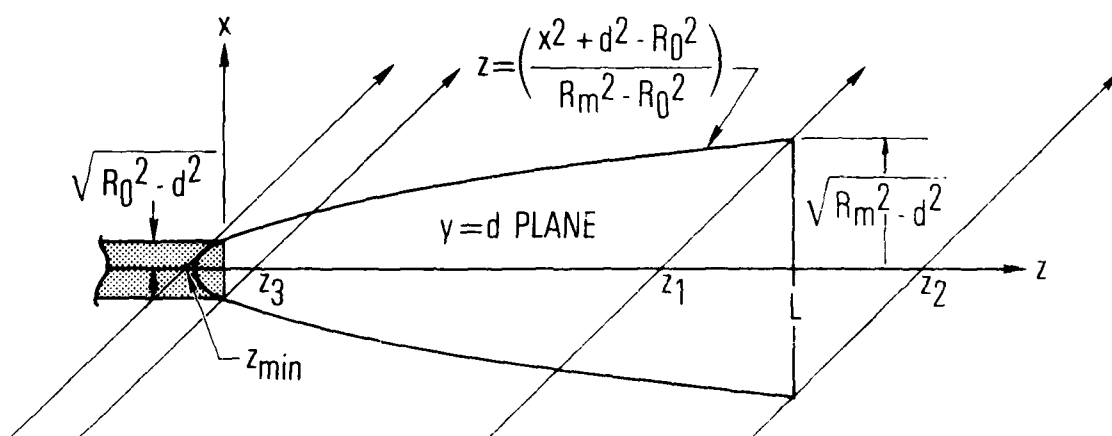


Figure 7. Axial Coordinate Test Points



Table 5. LOS - Plume Intersection Cases

Case	LOS Entrance Surface	LOS Exit Surface	$\alpha$	$z_0$	d	Entrance Coordinate		Exit Coordinate	
						$X_1$	$Z_1$	$X_2$	$Z_2$
1	Control	End	$\alpha < \pi/2$	$z_0 > z_3 \left\{ \begin{array}{l} \text{if } d < R_0 \\ z_1 < z_0 < z_2 \end{array} \right.$		$x_-$	$z_-$	$x_e$	L
2	Control	Control		$z_0 > z_3 \left\{ \begin{array}{l} \text{if } d < R_0 \\ z_0 < z_1 \end{array} \right. \left\{ \begin{array}{l} \text{if } \alpha < \pi/2 \\ z_0 > -z_3 \end{array} \right. \left\{ \begin{array}{l} \text{if } d < R_0 \\ z_0 < z_3 \\ z_0 < z_1 \end{array} \right. \left\{ \begin{array}{l} \text{if } \alpha > \pi/2 \end{array} \right.$		$x_-$	$z_-$	$x_+$	$z_+$
3	Control	Nozzle	$\alpha > \pi/2$	$z_3 < z_0 < -z_3$ $z_0 < z_2$	$d < R_0$	$x_-$	$z_-$	$x_n$	0
4	End	Control	$\alpha > \pi/2$	$z_0 > -z_3 \left\{ \begin{array}{l} \text{if } d < R_0 \\ z_0 < z_3 \end{array} \right.$ $z_2 < z_0 < z_1$		$x_e$	L	$x_+$	$z_+$
5	End	Nozzle	$\alpha > \pi/2$	$z_3 < z_0 < -z_3$ $z_2 < z_0 < z_1$	$d < R_0$	$x_c$	L	$x_n$	0
End-on Aspects	Control	End	$\alpha = 0$		$d > R_0$	d	d	$z_C$	L
	End	Control	$\alpha = \pi$		$d > R_0$	d	d	L	$z_C$
	End	Nozzle	$\alpha = \pi$		$d < R_0$	d	d	L	0

$$x_e = (L - z_o) \tan \alpha \quad \text{entrance or exit on end-plane}$$

$$x_n = -z_o \tan \alpha \quad \text{exit on nozzle-plane}$$

$$z_c = L \left( \frac{d^2 - R_o^2}{R_m^2 - R_o^2} \right) \quad \text{entrance or exit on control surface } (\alpha = 0, \pi)$$

With these coordinates defined, the total length of the path through the plume is computed from

$$s_{\max} = \sqrt{(X_1 - X_2)^2 + (Z_1 - Z_2)^2}$$

The total length of the path within the plume is divided into N equal size intervals and an array of path position defined by

$$s(i) = (i - 1) \frac{s_{\max}}{N} \quad i = 1, N + 1$$

Arrays of radial and axial coordinates corresponding to each value of i are computed from

$$\left. \begin{aligned} r(i) &= \sqrt{[X_1 + s(i) \sin \alpha]^2 + d^2} \\ z(i) &= Z_1 + s(i) \cos \alpha \end{aligned} \right\} \quad i = 1, N + 1$$

For  $i = 1$ ,  $s(i) = 0$  and  $r(i)$ ,  $z(i)$  are the cylindrical coordinates of the entrance point of the LOS. For  $i = N + 1$ ,  $s(i) = s_{\max}$  and  $r(i)$ ,  $z(i)$  are the coordinates of the exit point.

Values of  $pTc$  for each point ( $i = 1, N + 1$ ) along the path are computed by linear interpolations based on the input plume  $pTc$  data and the coordinates  $r(i)$ ,  $z(i)$ . The plume data  $f(n, m)$  [ $f$  represents  $p$ ,  $T$ , or any  $c$ ] are defined on the grid

$zz(n) \dots n = 1, NZ \dots$  axial stations

$rr(n, m) \dots m = 1, NR(n) \dots$  radial stations at each  
 $n = 1, NZ$  axial station

The first step of the interpolation procedure is the location of the axial stations  $z_1 = zz(n)$ ,  $z_2 = zz(n + 1)$  bounding  $z(i)$ , i.e.,  $z_1 < z(i) < z_2$ . The procedure now diverges depending on whether  $r(i) \leq r_1$  or  $r(i) > r_1$  where  $r_1$  is the maximum grid radius at  $z_1$ ,  $r_1 = rr[n, NR(n)]$ . For  $r(i) \leq r_1$  (case 1), the radial stations at  $z_1$  and  $z_2$  that bound  $r(i)$  are determined and intermediate interpolations performed to get the function  $f$  at the points  $z_1$ ,  $r(i)$  and  $z_2$ ,  $r(i)$  as shown in Figure 8. An axial interpolation is then performed using  $f_1$ ,  $f_2$ ,  $z_1$ ,  $z_2$ , and  $z(i)$  to get  $f$  at  $z(i)$ ,  $r(i)$ . This interpolation procedure can be interpreted as a construction of the  $f$ -surface by the drawing of straight lines between the  $f$  profiles at  $z_1$  and  $z_2$ , the lines being equally spaced in  $r$  out to  $r_1$  (see Figure 9). The interpolation procedure for  $r > r_1$  (case 2) is based on the completion of the  $f$ -surface construction by the drawing of straight lines from the point  $r_1$  that fan out to the  $f$ -profile at  $z_2$  (see Figure 9). The interpolation for case 2 based on this  $f$ -surface construction proceeds by computing the radial parameter (see Figure 10),

$$r_o = r_1 + \frac{r(i) - r_1}{z(i) - z_1} (z_2 - z_1)$$

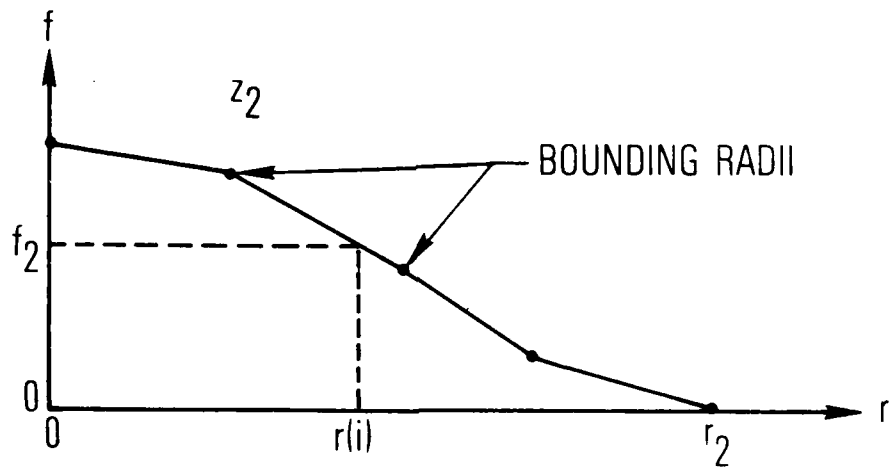
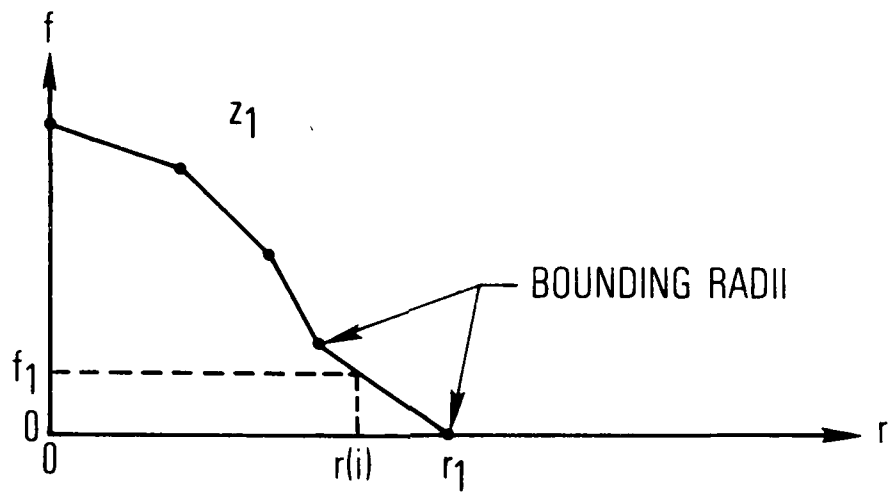


Figure 8. Intermediate Interpolation for Case 1

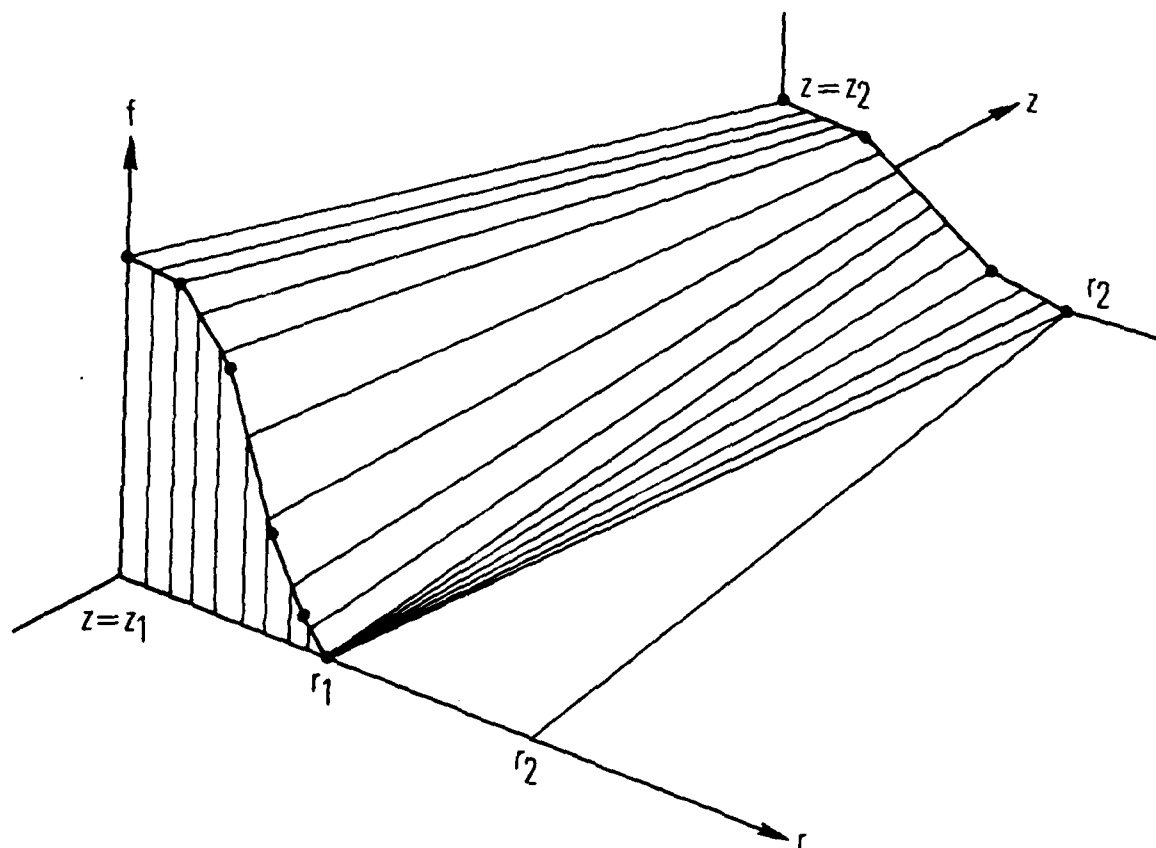


Figure 9. Interpolation Surface

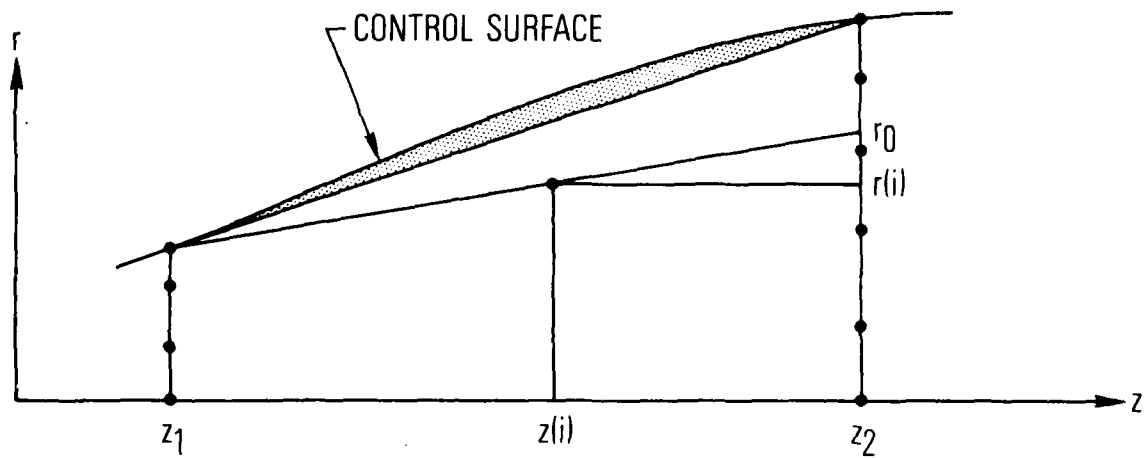


Figure 10. Case 2 Interpolation Geometry

and performing an intermediate interpolation for  $f_2$  at the point  $z_2, r_o$ . An axial interpolation is then made for the final value of  $f$  at  $r(i), z(i)$  by

$$f = f_1 + (f_2 - f_1) \frac{y}{y_m}$$

where

$$f_1 = f[n, NR(n)] = \text{plume boundary value}$$

$$y = \sqrt{[z(i) - z_1]^2 + [r(i) - r_1]^2}$$

$$y_m = \sqrt{(z_2 - z_1)^2 + (r_o - r_1)^2}$$

If the computed value of  $r_o$  is greater than the plume radius at  $z_2$ , i.e.,  $r_2 = rr[n + 1, NR(n + 1)]$ , then the point  $z(i), r(i)$  lies in the shaded area shown in Figure 10. Although the point is inside the plume control volume, the value of  $f$  is set to the plume boundary value,  $f_1$ .

#### E. Subroutine DELTRAN

Subroutine DELTRAN is the primary band model calculation routine. The input consists of arrays of pTc data and band model parameters describing an optical path. Specifically, the following arrays are entered

$s(i)$	path position (cm), $s(i) = 0$	} $i = 1, N + 1$
$p(i)$	pressure (atm)	
$c(i)$	concentration (mole fraction)	
$\bar{k}(i)$	absorption parameter ( $\text{cm}^{-1}/\text{atm}$ )	
$D(i) = 1/\delta(i)$	line density ( $1/\text{cm}^{-1}$ )	
$\bar{\gamma}_L(i)$	Lorentz line width parameter ( $\text{cm}^{-1}$ )	
$\gamma_D(i)$	Doppler line width parameter ( $\text{cm}^{-1}$ )	

Mode data are also entered to indicate line shape and inhomogeneity approximation to be used. The return of the subroutine are the transmittance  $\bar{\tau}(i)$  and transmittance derivative  $d\bar{\tau}(i)/ds$  for a single species. The method of computation has been given in Section II. Path integrals appearing in the band model formulation are computed by trapezoidal quadrature on the coordinate axis  $s(i)$ .

For a given species, three calls to DELTRAN are made by the main program ATLES. The first call computes  $\bar{\tau}(i)$  and  $d\bar{\tau}(i)/ds$  along the absorption path. For these calculations the initial values of path integrals are set to zero at  $i = 1$ . When the calculation loop ends at  $i = N + 1$ , the cumulative sums representing the path integrals over the entire absorption path are saved. The second call to DELTRAN computes  $\bar{\tau}(i)$  and  $d\bar{\tau}(i)/ds$  over the emission portion of the total optical path as though the absorption path were not present. This calculation is carried out by again initiating integral sums to zero at  $i = 1$ . The cumulative sums for this calculation are not saved. The third call to DELTRAN computes  $\bar{\tau}(i)$  and  $d\bar{\tau}(i)/ds$  over the emission path, but this time with account of absorption by the coupled absorption path. This calculation is performed by initializing the path integrals at  $i = 1$  to the cumulative sums that have been saved from the first call to DELTRAN.



#### IV. PREPARATION OF INPUT DATA

A computational run of ATLES requires a set of program control cards (Figure 11) to specify the mode of computation and to supply input data. A control card may also signal that auxiliary data are to be read in by the program. These auxiliary data may be provided in card-deck form or as attached tape or disc files. When the set of control cards and auxiliary data are read in, a computational run is made and an output listing is generated. The program then continues to read a new set of program control cards and execute a new run. The computations of the second and subsequent runs proceed with the conditions of the first run as modified by changes indicated by the subsequent control cards.

Each type of control card contains an alphanumeric name in the first ten card columns, and must be left-justified. If data are specified on the control card, they must be entered in accord with the format specification indicated in the detailed descriptions given below. All fields of the program control cards are 10 columns wide. In general, integer and alphanumeric (Hollerith) data must be right-justified in their fields. Noninteger numerical data may be entered in either F-format with decimal point or right-justified E-format with decimal point and exponential symbol E. The types of control cards and the data contained on them are illustrated in Figure 11. Detailed descriptions of each card type are given in the following sections.

- A. Title Card: The card name is TITLE. Columns 11-60 of this card may be used for any identification title desired. The title will be displayed in the final listing of the computation run and on any plots generated by the run.
- B. Calculation Mode Card: The card name is CALCMODE. The variable CMODE (format A10) must have one of the three alphanumeric values ATM, SRC, or CPL. The value ATM signals that calculation for an absorption path only will be made. This mode would be used, for example, in computing the transmittance spectrum over an atmospheric slant path. Similarly, the value SRC indicates that

	10	20	30	40	50	60	70	80
TITLE								
CALCMODE	CMODE	LSHAPE						
INTERVALS	NAPATH	NSPATH	DELS					
INHOMMODE	MODEATM	MODESRC	MODECPL					
SPECTRUM	UNIT	WMIN	WMAX	NSPEC				
BANDPASS	WL	WU						
GEOMETRY	PCODE	ZMAX	ALT	ZENITH	RANGE	ASPECT		
PRINT	WATM	WSRC						
PLOTRAD	WSCALE	CSRC	CSNSR	CATM				
PLOTTRAN	WSCALE	CT	CTE					
SPECIES	SNAME	SNUMBER	NFILE	PRINT				
ATMOSPHERE	ACODE	NFILE	PRINT	C1	C2	C3		
SOURCE	SCODE	NTAPE	PRINT	C1	C2	C3		
GRID		Z	D					
GRID	NTAPE	PRINT	WMAP					
RUN								

Figure 11. Program Control Card Formats

calculations for an emission path only will be made. If the value is CPL, full calculations for a coupled emission/absorption optical path are performed. If the emission source is specified as a plume (see SOURCE card) and the absorption path as an atmospheric slant path (see ATMOSPHERE card), for example, calculations would be made for:

1. Plume radiance at plume boundary
2. Plume radiance attenuated by atmosphere
3. Transmittance (and radiance) of atmospheric slant path
4. Effective atmospheric slant path transmittance

The variable LSHAPE (format A10) on the CALCMODE card defines the spectral line shape that will be used in the statistical band model calculations. This variable must have one of the three alphanumeric values LORENTZ, DOPPLER, or VOIGT. For calculations involving atmospheric slant paths, the use of the Lorentz line profile is generally adequate if one end of the slant path is below  $\sim 20\text{km}$ .

- C. Path Intervals Card: The card name is INTERVALS. The variables NAPATH and NSPATH (each format I10) are the number of equal geometric length intervals into which the absorption and emission path,\* respectively, are divided for numerical integrations over the paths. The minimum allowed value of either variable is one and the maximum allowed value is 100. The value of these two variables must be large enough to give reasonable numerical accuracy, but, in order to minimize computer cost, should not be too much larger than necessary. For a large run in which calculations will be made for many lines of sight through a plume for many spectral positions, an empirical determination of NAPATH and NSPATH can be made for one line of sight at one spectral position (see discussion of SPECTRUM and GRID program control cards). The spectral position selected should be one for strong absorption and the line of sight should be one which passes through the plume where the optical density is large. Then, by making a series of runs with

---

\* Except, an equal mass division is made for atmospheric slant paths.

increasing NAPATH and NSPATH, optimum values can be determined by noting how the computed results converge.

For problems involving a plume source, it may not be desirable to use a fixed value for NSPATH. A fixed value implies that the portion of the line of sight through the plume is divided into the same number of integration intervals whether the line of sight passes through a full diameter of the plume or just grazes the boundary. In the former case, a large value of NSPATH may be required whereas in the latter, a value near one would probably be sufficient. An effective variable value of NSPATH can be used for such plume calculations by setting NSPATH to zero (or blank) and specifying the approximate source path increment directly. This increment (unit = m) is entered as DELS (format E10) on the interval card. Integrations along the source portion of the line of sight will be made with an integration interval approximately equal to DELS regardless of the length of the optical path through the plume.

For calculations involving absorption or emission cells (see SOURCE and ATMOSPHERE cards) NAPATH and NSPATH may be set (appropriately) to zero. In this case, equal divisions along the optical path segments are not made, but rather the coordinates used to enter the pTc data along the path segments are used to define the integration interval subdivision.

- D. Inhomogeneity Approximations Card: The card name is INHOMMODE. The variables MODEATM, MODESRC, and MODECPL specify the approximation that will be used to handle nonuniformities along the absorption, emission, and coupled absorption/emission paths, respectively. The format of each is A10, and the allowed values are UNIFORM, CG and DR. The value CG indicates that the Curtis-Godson approximation will be used while DR indicates that the derivative approximation will be used. MODEATM = CG is adequate for atmospheric slant paths and may be adequate for

computing source radiance if thermal gradients are not too large. For large thermal gradients within the source, MODESRC should be set to DR. Computation of hot gas emission attenuated by an intervening atmospheric path should almost always be made with MODECPL = DR.

The value UNIFORM indicates that calculations will be made as though the path were uniform, and is an appropriate value only for MODEATM and MODESRC. If MODEATM and/or MODESRC have this value, an override of the values NAPATH and/or NSPATH on the INTERVALS card is made and calculations are made as though they had been specified as one. The entered value of NSPATH still gives the subdivision of the source path segment used for the coupled-path calculation.

- E. Spectrum Card: The card name is SPECTRUM. The variable UNIT (format A10) determines the spectral units required for input spectral data and also the spectral unit of computed results. If UNIT has the value MICRON, input spectral data must be in  $\mu\text{m}$ , and computed radiance results will be expressed in  $\text{W}/\text{cm}^2\text{-sr-}\mu\text{m}$  as a function of wavelength in  $\mu\text{m}$ . If UNIT has any other value, spectral data must be entered as wavenumber with unit  $\text{cm}^{-1}$ . Computed radiance spectra will be listed with unit  $\text{W}/\text{cm}^2\text{-sr-cm}^{-1}$  as a function of wavenumber with unit  $\text{cm}^{-1}$ .

The variables WMIN and WMAX are the lower and upper extent, respectively, of the spectral region to be considered. The format specification of each is E10 and the unit must correspond to UNIT. The region between WMIN and WMAX is divided into NSPEC (format I10) equal-size intervals and calculations performed at the resulting NSPEC + 1 spectral positions. The minimum and maximum allowed values for NSPEC are 0 and 200, respectively. If NSPEC is 0, calculations at only the one spectral position WMIN are made.

- F. Bandpass Card: The card name is BANDPASS. The variables WL and WU (each format E10) are the lower and upper extents, respectively, of a spectral bandpass over which the computed radiance and transmittance spectra will be averaged. In order to be meaningful, these limits should be the same, or inside, the spectral limits set by the SPECTRUM card. The BANDPASS card can be used to compute average spectral values within a specified sensor bandpass if the inband responsivity of the sensor is assumed to be constant. Up to 10 different BANDPASS cards may be used in one computational run. The unit of WL and WU must be consistent with the value of UNIT on the SPECTRUM card.

The BANDPASS card may also be used to eliminate all previously defined bandpasses by giving WL the alphanumeric value RESET.

- G. Geometry Card: The card name is GEOMETRY and is used to define the geometry of observation along an atmospheric slant path. This geometry may be defined in one of two ways.

If PCODE (format A10) has the value EXOATM, the geometry consists of a sensor above the atmosphere looking down on a target plume within the atmosphere (see Figure 3). In this case, the variable ALT (format E10) is the altitude of the target plume above ground level (unit = km), and ZENITH (format E10) is the zenith angle (unit = degrees) from the plume to the sensor (ZENITH = 0 implies that the sensor is directly above and looking down on the target).

If PCODE has the value ENDOATM, the geometry is defined with reference to a sensor within the atmosphere (see Figure 4). The emission source may be either within or above the atmosphere. In this case, ALT is the sensor altitude and ZENITH is the zenith angle from the sensor to the source (ZENITH = 0 implies that the sensor is directly below and looking up at the source). The variable RANGE (format E10) is the range in km from the sensor to the target and needs to be defined only if PCODE = ENDOATM.

The variable ZMAX (format E10) defines the "top of the atmosphere" and may be any value less than or equal to 100km. The unit is km.

If the emission source is a plume (see SOURCE card), the variable ASPECT (format E10) is used and is the viewing angle between the plume axis and the line of sight. The unit is degrees, and the angle is measured from nose-on to the missile or aircraft generating the plume.

- H. Print Card: The card name is PRINT and contains the two variables WATM and WSRC (each format A10). If WATM has the value PRINT, a detailed printout of all major computational steps throughout the program for the absorption path portion of the total optical path results. Similarly, if WSRC = PRINT, printouts for the source portion occur. The use of this card should be restricted to debugging or computational check runs only. If any more than one spectral position for one line of sight is involved in the job run, the printout will be enormous.
- I. Plot Cards<sup>\*</sup>: The two cards named PLOTTRAD and PLOTTRAN specify if any film plots are to be made of the computed radiance and transmittance spectra, respectively. The variable WSCALE (format E10) is the spectral plot scaling parameter and has unit  $\text{cm}^{-1}/(\text{inch of plot})$  or  $\mu\text{m}/(\text{inch of plot})$  depending on the value of UNIT on the SPECTRUM card. The value of WSCALE should be chosen so that the entire spectral interval specified by the SPECTRUM card is contained within a 12-inch plot. Note that WSCALE is included on both the radiance and transmittance plot cards. The last value of WSCALE read is the value used.

---

<sup>\*</sup>This description is of concern only to users at The Aerospace Corporation since the plot functions used in the coding are in-house routines. Users outside The Aerospace Corporation must write their own plot routine.

If a PLOTTRAD card is included in the input, but CSRC, CSNSR and CATM are not specified (normal usage), the following radiance plots will be generated.

1. Source radiance with an optimum y-scale factor
2. Sensor radiance (attenuated source radiance) with an optimum y-scale factor
3. Sensor radiance with the same y-scale factor as plot one (but only if the factor is different from that for plot two)
4. Atmospheric radiance with an optimum y-scale factor
5. Atmospheric radiance with the same y-scale factor as plot one (but only if the factor is different from that for plot four)

If CSRC, CSNSR or CATM (each format E10) are specified, additional plots for the source, sensor, or atmospheric radiance, respectively, are generated using these values as the y-scaling factors. The unit of these variables is (spectral radiance consistent with UNIT)/(inch of plot). If CSRC, CSNSR or CATM are the same as the scale factor for any of the five basic radiance plots, no additional plots are made. The maximum allowed plot height is 10 inches.

The PLOTTRAN card operates in a similar manner. The basic transmittance plots are

1. Atmospheric transmittance with a y-scale factor of 0.10
2. Effective atmospheric transmittance with a y-scale factor of 0.10

If CT and CTE are not zero, additional transmittance plots are made for the atmospheric and effective atmospheric transmittances, respectively, using these values as the y-scale factor. The unit of CT or CTE is (full scale percent transmittance/1000)/(inch of plot) for a 10 inch high plot.



- J. Species Card: The card name is SPECIES and is used to include a particular molecular species in the calculations and to call for the input of band model parameters for that species. SNAME (format A10) is an arbitrary identification name for the species (e.g., H<sub>2</sub>O, CO<sub>2</sub>, N<sub>2</sub>O) and SNUMBER (format I10) is an identification number (allowed values are 1, 2 or 3). If SNAME has the value DELETE, the species identified by SNUMBER is deleted from current and subsequent calculations. If NFILE is zero or blank, band model parameters for the species must follow the SPECIES card immediately in the input card file. The required deck structure is given in Figure 12. If NFILE is not zero, then the value specifies the section on the Band Model Parameter File containing the desired parameters. This file must have been attached to the job run on input device labeled 2<sup>\*</sup>. The band model parameter section identification numbers are given in Table 2. If the variable PRINT (A10) has the value PRINT, a listing of the band model parameters will be made. Up to three SPECIES cards (with different SNUMBER) may be used in one computational run.
- K. Atmosphere Card: The card name is ATMOSPHERE. The variable ACODE (format A10) must be one of the three values ATM, LOS or NOREAD. The value ATM indicates that the absorption path is an atmospheric slant path and that data specifying the altitude profile of a model atmosphere should now be made available. If NFILE (format I10) is blank or zero, the model atmosphere data is assumed to be in card deck form and to immediately follow the ATMOSPHERE control card. The required deck structure is given in Figure 13. If NFILE is not zero, the value indicates the section of the Model Atmosphere File that contains the desired model. This file must have been previously attached to the job on input device 3<sup>\*</sup>.

---

\* For the CDC 7600 computer with SCODE 3 operating system, the Band Model Parameter File must have been attached to the job with file name TAPE2 and the Model Atmosphere File with file name TAPE3.

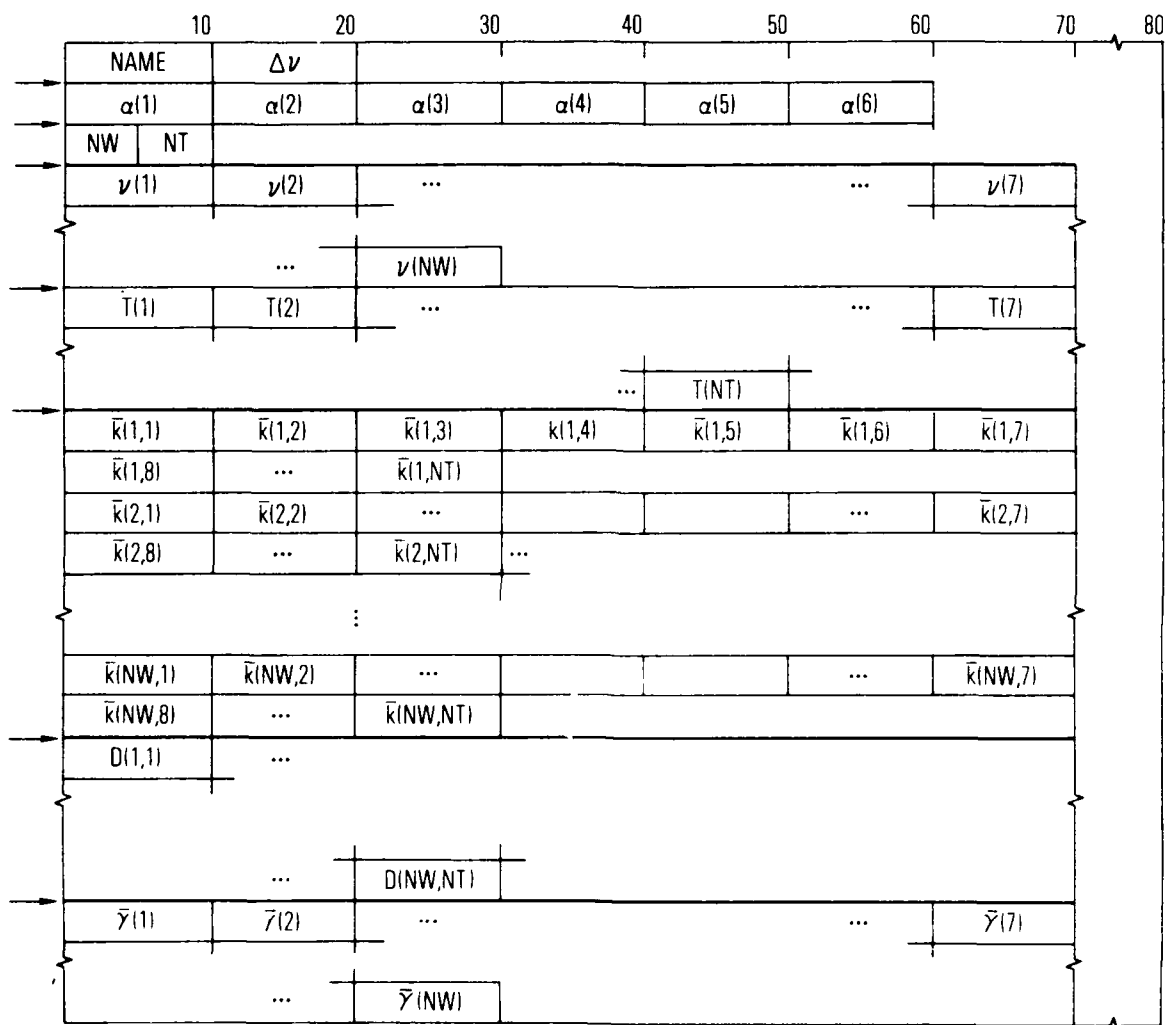


Figure 12. Band Model Parameter Set Deck Structure

## LEGEND

NAME	Identification name (format A10)*
$\Delta\nu$	Spectral resolution of data ( $\text{cm}^{-1}$ ) <sup>†</sup>
$\alpha(1)$	Ratio of resonant self-broadening parameter to $\bar{\nu}$
$\alpha(2)$ <sup>‡</sup>	Ratio of $\text{H}_2\text{O}$ foreign gas broadening parameter to $\bar{\nu}$
$\alpha(3)$ <sup>‡</sup>	Ratio of $\text{CO}_2$ foreign gas broadening parameter to $\bar{\nu}$
$\alpha(4)$	Ratio of $\text{N}_2$ foreign gas broadening parameter to $\bar{\nu}$
$\alpha(5)$	Ratio of $\text{O}_2$ foreign gas broadening parameter to $\bar{\nu}$
$\alpha(6)$	Mass of absorbing species (amu)
NW	Number of elements in wavenumber array (format I5)
NT	Number of elements in temperature array (format I5)
$\nu(i)$	Wavenumber array ( $\text{cm}^{-1}$ ) $i = 1, 2, 3, \dots, \text{NW}$
$T(j)$	Temperature array ( $^{\circ}\text{K}$ ) $j = 1, 2, 3, \dots, \text{NT}$
$K(i, j)$	Mean absorption coefficient array ( $\text{cm}^{-1}/\text{atm}$ )
$D(i, j)$ <sup>§</sup>	Effective line density parameter array ( $1/\text{cm}^{-1}$ )
$\bar{\nu}(i)$	Broadening parameter for non-resonant self-broadening at STP ( $\text{cm}^{-1}/\text{atm}$ )

\* Unless otherwise indicated, as here, all fields are format E10 and data contain appropriate decimal points and exponential symbols E.

<sup>†</sup> The interval size between elements of the  $\nu(i)$  array may be  $\Delta\nu$  also, but need not be.

<sup>‡</sup> If the parameter set is for  $\text{H}_2\text{O}$ ,  $\alpha(2) = 0$ . If for  $\text{CO}_2$ ,  $\alpha(3) = 0$ .

<sup>§</sup>  $D(i, j) \equiv 1/\bar{\delta}(i, j)$ . This parameter is the effective line density parameter consistent for use in the statistical band model for equal strength lines.

Figure 12. Band Model Parameter Set Deck Structure

10		20		30		40		70		80	
IDNAME		IUNIT									
h(1)	p(1)		T(1)	c <sub>H2O</sub> (1)							
h(2)	p(2)		T(2)	c <sub>H2O</sub> (2)							
⋮	⋮		⋮	⋮							
h(33)	p(33)		T(33)	c <sub>H2O</sub> (33)							
6		16		22		32					

IDNAME                      model atmosphere identification name  
(NAME is optional, but card must be included)

h(i)                          altitudes (m). h(i) must be the 33 values  
0, 1, 2, . . . , 24, 25, 30, 35, 40, 45, 50, 70, 100 km.

T(i)                          temperature (K)

IUNIT                        units flag

If IUNIT = 1                p(i) - pressure (atm)  
c<sub>H<sub>2</sub>O</sub>(i) - water vapor concentration  
(mole fraction)

If IUNIT ≠ 1                p(i) - pressure (mb)  
c<sub>H<sub>2</sub>O</sub>(i) - water vapor concentration (g/m<sup>3</sup>)

Figure 13. Deck Structure for Model Atmosphere  
Input Data.

The section identification numbers are given in Table 1. If the variable PRINT (format A10) has the value PRINT, the model atmosphere data will be listed. The variables C1, C2 and C3 are used to specify concentration conditions for species identified as 1, 2 and 3, respectively, by the SPECIES cards. If  $C_i$  is zero or blank (format E10), species  $i$  is not considered as an atmospheric constituent. If  $C_i$  has a numerical value (format E10) this value will be used as the constant mixing ratio of species  $i$  in the atmosphere. If  $C_i$  has the value H2O (format A10), the water vapor concentration profile of the model atmosphere will be used to determine concentrations for species  $i$ .

A user may specify the pressure, temperature and species concentration (pTc) along an absorption line of sight by setting ACODE to the value LOS. In this case, NTAPE should be set to five and a card deck of the pTc data inserted immediately after the ATMOSPHERE card. The required input card deck structure is given in Figure 14. If PRINT has the value print, this pTc data will be listed. The pTc deck allows for the specification of up to five species. The variables  $C_i$  (format I10) in this case identify the "species column" containing the concentration data to be assigned to species  $i$ . "Species column" is defined by: species column 1 = card columns 31-40, species column 2 = card columns 41-50, ..., species column 5 = card columns 71-80. For example, if species 2 has been identified by the SPECIES card to be CO, and the CO concentration has been entered on the pTc data deck in card columns 61-70, then  $C_2 = 4$ .

The value ACODE = NOREAD, indicates that neither an atmospheric model nor a pTc data deck is to be read in (presumably one of these having been read in on a previous run), but that new data assignments are to be made by a new set of  $C_i$  variables.

- L. Source Card: The card name is SOURCE and operates in much the same way as the ATMOSPHERE card does. SCODE (format A10) may be one of the three values PLM, LOS or NOREAD. The first

10	20	30	40	50	60	70	80
IDNAME	N		NAME1	NAME2	NAME3	NAME4	NAME5
s(1)	p(1)	T(1)	c <sub>1</sub> (1)	c <sub>2</sub> (1)	c <sub>3</sub> (1)	c <sub>4</sub> (1)	c <sub>5</sub> (1)
s(2)	p(2)	T(2)	c <sub>1</sub> (2)	c <sub>2</sub> (2)	c <sub>3</sub> (2)	c <sub>4</sub> (2)	c <sub>5</sub> (2)
⋮	⋮	⋮	⋮	⋮	⋮	⋮	⋮
s(N)	p(N)	T(N)	c <sub>1</sub> (N)	c <sub>2</sub> (N)	c <sub>3</sub> (N)	c <sub>4</sub> (N)	c <sub>5</sub> (N)

IDNAME                      cell identification name (optional)

N                              number of path positions for which data is to be entered.  $2 \leq N \leq 101$  and N is integer

NAME1 thru NAME5            species identification names (optional)

s(i)                            path positions. s(1) = 0 and s(i) increases with i

p(i)                            pressure (atm)

T(i)                            temperature (K)

c<sub>m</sub>(i)                        species concentrations (mole fraction).  
 $1 \leq m \leq 5$

Figure 14. Deck Structure for Emission or Absorption Cell Input Data

value indicates that the radiation source to be considered is a plume and the second that the source is a single line of sight through a hot gas region. The nominal input mode for the plume or line of sight pTc data is a card deck immediately following the SOURCE card. The structures for the line of sight and plume pTc data decks are given in Figures 14 and 15, respectively. For card input, NTAPE (format I10) must be 5. If the pTc data are attached to the job in tape or permanent file form, they should be attached on input device i and NTAPE set to i. A value i = 7, 8 or 9 is allowed. If PRINT (format A10) has the value PRINT, the pTc input data will be listed. The parameters C1, C2 and C3 (each format I10) are the species column in which the concentration data for species 1, 2 and 3, respectively, are entered in the pTc data deck. The value SCODE = NOREAD is used when only the species column assignment is to be changed.

- M. Plume Integration Card: The CARD name is GRID and is used to specify how the integration over the projected area of a plume is to be performed. Two forms of the card are allowed. If calculations for a single line of sight through a plume are desired, the NTAPE field (format I10) should be left blank. The line of sight is then defined by the axial distance Z (format E10 and unit = m) from the nozzle and the transverse distance D (format E10 and unit = m) from the plume axis of the point of intersection between the line of sight and the projected area of the plume. If NTAPE = i (format I10) is not blank, the Z and D coordinates defining many lines of sight through the plume will be read in from input device i. If NTAPE = 5, the grid data must be in card deck form and immediately follow the GRID card. The required deck structure is given in Figure 16. If the variable PRINT (format A10) has the value PRINT, the grid data will be listed. If the variable WMAP (format A10) has the value PRINT, the computational results of the bandpass averaged radiance and transmittance for each line of sight through the plume will be listed. (The normal output is the area averaged result for all the lines of sight.)

10	IDNAME	L	R <sub>0</sub>	R <sub>m</sub>	NZ	NAME1	NAME2	NAME3	NAME4	NAME5	70	80
	Z(i)	NR(i)										
	r(i,1)	p(i,1)	T(i,1)	c <sub>1</sub> (i,1)	c <sub>2</sub> (i,1)	c <sub>3</sub> (i,1)	c <sub>4</sub> (i,1)	c <sub>5</sub> (i,1)				
	r(i,2)	p(i,2)	T(i,2)	c <sub>1</sub> (i,2)	c <sub>2</sub> (i,2)	c <sub>3</sub> (i,2)	c <sub>4</sub> (i,2)	c <sub>5</sub> (i,2)				
	:	:	:	:	:	:	:	:	:	:		
	r(i, NR(i))	p(i, NR(i))	T(i, NR(i))	c <sub>1</sub> (i, NR(i))	c <sub>2</sub> (i, NR(i))	c <sub>3</sub> (i, NR(i))	c <sub>4</sub> (i, NR(i))	c <sub>5</sub> (i, NR(i))				

DECK STRUCTURE FOR i<sup>th</sup> AXIAL STATION  
STRUCTURE IS IDENTICAL FOR ALL i = 1,NZ

Figure 15. Deck Structure for Plume Input Data



## LEGEND

IDNAME	plume identification name (optional)
L	control volume length (m)
$R_o$	nozzle radius (m)
$R_m$	maximum control volume radius (m)
NZ	number of axial stations for which data is to be entered. $2 \leq NZ \leq 31$ and NZ is integer
NAME1 thru NAME5	species identification names (optional)
Z(i)	axial station positions (m). Note: $Z(1) = 0$ (exit plane), $Z(NZ) = L$ , and $Z(i)$ increases with i
NR(i)	number of radial stations at axial station i. $2 \leq NR(i) \leq 11$ and NR(i) is integer
r(i, j)	radial station positions (m). Note: $r(i, 1) = 0$ (axis). $r[i, NR(i)] = \sqrt{\frac{Z(i)}{L} (R_m^2 - R_o^2) + R_o^2}$ , r(i, j) increases with j
p(i, j)	pressure (atm). If $p(1, 1) = 0$ , the ambient atmospheric pressure at the plume altitude is used for all p(i, j)
T(i, j)	temperature (K)
$c_m(i, j)$	species concentrations (mole fraction). $1 \leq m \leq 5$
Note: The boundary values of p(i, j), T(i, j) and $c_m(i, j)$ [i.e., for j = NR(i)] should be set to the ambient atmospheric values.	

Figure 15. Deck Structure for Plume Input Data

10	20	30	40	50	60	70	80
IDNAME	NZ						
Z(i)	ND(i)	D(i,1)	D(i,2)	D(i,3)	D(i,4)	D(i,5)	D(i,6)
D(i,7)	D(i,8)						

IDNAME                      grid identification name (optional)

NZ                            number of axial grid coordinates where LOS calculations will be made.  $1 \leq NZ \leq 21$  and NZ is integer

Z(i) \*                        axial grid coordinate (m). Z(i) increases with i

ND(i)                         number of transverse grid coordinates at axial coordinate i.  $1 \leq ND(i) \leq 8$

D(i, j)                        transverse grid coordinates (m). D(i, j) increases with j. If  $ND(i) \leq 6$ , delete second card

This coordinate is measured in the plume coordinate system, not the projected area coordinate system. For aspect angles near 0 or 180°, negative values of Z may be required in order to properly specify the desired line of sight.

Figure 16. Deck Structure for Integration  
Grid Input Data

The following integration cases can be handled by a suitable combination of the GRID control card and auxiliary grid data.

Case 1. Single Line of Sight

In this case, only the GRID card (Type 1) is required. The coordinates  $Z(1)$  and  $D(1, 1)$  are obtained directly from the GRID card.  $NZ$  and  $ND(1)$  are automatically set to 1. If  $ASPECT = 0$  or  $180$  (see GEOMETRY card),  $Z(1)$  need not be specified.

Case 2. Single Axial-Station

The auxiliary grid data deck consists of one or two card with  $NZ$  specified as 1 and containing the  $D(1, j)$  values where computations are to be made. Note:  $D(1, 1)$  must be zero.

Case 3. Whole Plume Average ( $ASPECT \neq 0$  or  $180$ )

The full auxiliary data deck is required. Note:  $D(i, 1)$  must be zero for all  $i$ .

Case 4. Whole Plume Average ( $ASPECT = 0$  or  $180$ )

This case is the same as Case 2 except that  $Z(1)$  need not be specified, and  $D(1, 1)$  need not be zero. For example, if  $ASPECT = 0$ ,  $D(1, 1)$  should be set equal to the obscuration disc radius  $R_0$ .

For an integration over the whole projected area of a plume, prior calculations are recommended. Although the plume is defined throughout a paraboloid control volume, the area of integration specified by the grid data need not (and for economy's sake, should not) be the entire projected area of this volume. The integration area need be only the region where the majority of the radiation is emitted. A series of runs using the Type 1 GRID program control card with  $D(1, 1) = 0$  can be used to estimate the axial extent of the integration area. These computations can usually be done for one wavenumber. The transverse extent of the significant part of the plume at each axial station can be estimated from the input plume data profiles. Or, radiance profiles at a selected axial stations can be generated by a series of runs with the Type 1 GRID card with constant  $Z$  and increasing  $D$ .

When the desired extent of the plume integration area has been determined, a full area integration run can be done. The integration over the projected area of the plume uses a simple trapezoidal numerical quadrature routine. The grid should be structured with a spatial resolution fine enough to justify this approach.

The specification of how the spatial integration over the projected area of a plume should be carried out is the most tedious problem in data preparation, particularly for viewing aspect angles which are not either end-on or broadside. The basic problem is to choose a grid of points on the projected area of the plume that adequately covers the areas of dominant radiation, represents a fine enough mesh so that the numerical integration is accurate, and is limited enough so that the cost of computation is not excessive. Attempts to automate the selection of an integration grid have been made but the routines are not yet considered useful enough to be incorporated into the code. Thus, the specification of the integration grid is left to the user's discretion. An example grid selection is given in Section V.

- N. Execution Card: The card name is RUN. When a RUN card is encountered, computations are begun using the data entered up to that point, and an output listing of the results is made. When the computation and listing are completed, the program continues to read program control cards until a new RUN card is encountered. A new computation is then begun using all of the conditions and data of the previous run except those which have been changed, added or deleted by the intervening program control cards and auxiliary data decks. The process is repeated until an end-of-file card is encountered. With this feature, several different computational runs can be made with one job submission. Other than the necessity that all required data be entered before a RUN card is encountered and that auxiliary data in card form immediately follow the control card that calls for them, the program control cards may be in any order.

Great care should be taken in the preparation of input data since there are very few internal checks of data consistency. A general feature in data preparation is that, if particular data on a control card are not required, they need not be specified. If none of the data on a control card are required, that card need not be included.

## V. EXAMPLE CALCULATIONS

### A. ERIM Hot-through Cold H<sub>2</sub>O Spectra

An experimental study designed specifically to measure the radiance spectra of hot gases as viewed through cool absorption paths has recently been completed at ERIM.<sup>(12)</sup> These measurements provide quantitative data against which band model formulations can be tested. This example calculation illustrates the use of ATLES in predicting radiance spectra for experimental set-ups such as used by ERIM.

The ERIM runs considered are identified as 9R and 11MR. The hot emission source is a hot-gas cell containing H<sub>2</sub>O and N<sub>2</sub>. The optical path through the source is uniform with  $L = 60\text{cm}$ ,  $T = 1200^\circ\text{K}$ ,  $p = 0.10\text{ atm}$ , and  $c(\text{H}_2\text{O}) = 0.50$ . The radiation from the hot H<sub>2</sub>O in the  $2.7\text{-}\mu\text{m}$  band is viewed through a long cool absorption cell also containing only H<sub>2</sub>O and N<sub>2</sub>. The absorption path is uniform with  $L = 100\text{m}$ ,  $T \approx 300^\circ\text{K}$ ,  $p = 0.07\text{ atm}$ ,  $c = 0.0143$  (case 9R), and  $c = 0.143$  (case 11MR).

The control card and auxiliary data deck input for four radiance calculation runs is shown in Figure 17 and discussed below (numbers refer to indicated card groups in Figure 17).

1. The calculation is performed in the coupled mode with the Lorentz line shape.
2. Since the absorption path is uniform, NAPATH is set to 1 and MODEATM is set to UNIFORM. The emission path segment is also uniform, and computation of the unattenuated source radiance is made with an effective value NSPATH = 1 because MODESRC is indicated as UNIFORM. When the coupled path calculations are made, the emission path segment is divided into 10 integration intervals and the CG approximation is employed. The value NSPATH = 10 was

①	TITLE	ERIM RUN-9R	COUPLED HOT-THRU-COLD	CG-APPROX	
	CALC MODE	CPL	LORENTZ		
	INTERVALS	1			
②	INNMHODE	UNIFORM	UNIFORM	CG	
③	SPECTRUM	420	1200	56	
④	SOURCE	LOS	1		
⑤	ERIM-HOT	0.1	1200	1	0
⑥	AT 405 PHASE	0.1	1200	0.5	0
⑦	ERIM-34	LOS	420-33	H2O-1142	
⑧	100%	0.07	300	0.143	
⑨	RUN	ERIM RUN-9R	COUPLED HOT-THRU-COLD	DR-APPROX	
	TITLE	UNIFORM	UNIFORM	DR	
⑩	INNMHODE	UNIFORM	UNIFORM	DR	
⑪	RUN	ERIM RUN-11R	COUPLED HOT-THRU-COLD	DR-APPROX	
	TITLE	LOS	NOPEAD	2	0
	ATMOSPHERE				
	RUN	ERIM RUN-11R	COUPLED HOT-THRU-COLD	CG-APPROX	
	TITLE	UNIFORM	UNIFORM	CG	
	INNMHODE	UNIFORM	UNIFORM	CG	
	RUN				

Figure 17. Control Card and Auxiliary Data Input Deck for ERIM Hot-through-Cold H<sub>2</sub>O Spectra

determined empirically by repeated runs with increasing NSPATH at the single spectral position  $\nu = 3750 \text{ cm}^{-1}$  and noting the rate of convergence of the calculated radiance to a constant value.

3. The spectral region from 3000 to 4400  $\text{cm}^{-1}$  is covered with 56 equal size steps (25  $\text{cm}^{-1}$  wide).
4. Only  $\text{H}_2\text{O}$  is considered as an active species and is identified by the name  $\text{H}_2\text{O}$  and species number 1. The combined band model parameters for  $\text{H}_2\text{O}$  are used.
5. The source is specified as a single line of sight with the pTc data to be read from a card deck. Concentration data for  $\text{H}_2\text{O}$  will be taken from the first species column of the input pTc source deck.
6. The pTc data deck for the source immediately follows the SOURCE control card. Since the source is uniform, only two data cards are required to specify the path.
7. The absorption path is identified as a single line of sight with the pTc data to be read from the following input deck. Concentration data is to be taken from species column 1 for this run.
8. Compute radiance spectra for case 9R with the CG approximation.
9. The same case is rerun, but the attenuated source radiance is computed with the DR approximation.
10. Case 11MR is run by redefining the species column in the absorption pTc deck where the  $\text{H}_2\text{O}$  concentration is to be obtained. The DR approximation from the previous run is retained.
11. Case 11MR is rerun with the CG approximation.



This job run will result in four output listings. The listing for case 9R with the DR approximation is given in Figure 18. The computed radiance spectra for the four cases are compared with experimental spectra in Figure 19. A discussion of these comparisons is given in Ref. (13).

#### B. J57 - Jet Engine Plume

This example illustrates the use of ATLES for a detailed study of the infrared signature of a jet-aircraft plume in both the 2.7- and 4.3- $\mu\text{m}$  spectral regions and for aircraft-to-aircraft and space-to-aircraft detection geometries. The thermodynamic properties of the plume were obtained with the General Electric code SCORPIO II and represent the plume of a J-57 engine operating at full military power at an altitude of 32,000 ft (9.75km).<sup>\*</sup> The temperature and concentration profiles of  $\text{H}_2\text{O}$  and  $\text{CO}_2$  for the plume are shown in Figures 20 and 21, respectively, and are tabulated in the input data listing of Figure 22. The plume pressure is assumed constant throughout the plume and equal to the ambient pressure at 9.75km. A control volume with nozzle radius  $R_0 = 0.35\text{m}$ , length  $L = 5\text{m}$ , and maximum radius  $R_m = 1.50\text{m}$  is used to contain the plume.

Both  $\text{H}_2\text{O}$  and  $\text{CO}_2$  are considered as active plume and atmospheric species in the 2.7- $\mu\text{m}$  region. Only  $\text{CO}_2$  is considered active in the 4.3- $\mu\text{m}$  region. The calculations are carried through with a spectral unit of  $\text{cm}^{-1}$ . The spectral limits in the 2.7- $\mu\text{m}$  region are 3000 to 4200  $\text{cm}^{-1}$  with a step size  $\Delta\nu = 25 \text{ cm}^{-1}$  (NSPEC = 48). In the 4.3- $\mu\text{m}$  region, the limits are 2150 to 2400  $\text{cm}^{-1}$  with  $\Delta\nu = 5 \text{ cm}^{-1}$  (NSPEC = 50). Combined band model parameters are used and selected for a 25  $\text{cm}^{-1}$  spectral resolution in the 2.7- $\mu\text{m}$  region and 5  $\text{cm}^{-1}$

---

<sup>\*</sup>F. S. Simmons, The Aerospace Corp., El Segundo, Calif., private communication (March 1975).

\*\*\*\*\* PLUME RADIATION CODE/OUTPUT LISTING \*\*\*\*\*

JOB TITLE.....ERIM RUN-3R      COUPLED HOT-THRU-COLD      ON-APPROX

OPTICAL PATH MODELS  
 PATH CONFIGURATION.....COUPLED EMISSION SOURCE AND ABSORPTION PATH  
 ABSORPT. OF PATH TO NAME.....PRIM-9R  
 EMISSION PATH 1 NAME.....ERIM-HOT

SPECIES DATA  
 SPECIES NUMBER.....1      2      3  
 SPECIES NAME.....H2O  
 PARAMETER SET TO NAME.....COUPLH2O  
 STATUS AS ABSORBER.....ON  
 STATUS AS EMITTER.....ON

SPECTRAL DATA  
 LOWER WAVELENGTH (CM-1).....1.000E+03  
 UPPER WAVELENGTH (CM-1).....4.400E+03  
 NUMBER OF INTERVALS.....56  
 WAVELENGTH INCREMENT (CM-1).....2.500E+01

PATH INTEGRATION DATA  
 NUMBER OF INTERVALS (ABSORPTION PATH).....1 (EQUAL LENGTH)  
 NUMBER OF INTERVALS (EMISSION PATH).....1 (EQUAL LENGTH)

SAND MODEL CALCULATION MODE  
 LINE SHAPE.....LCRINT7  
 INHOMOGENEITY MODES.....UNIFORM  
 ABSORPTION PATH.....UNIFORM  
 EMISSION PATH.....UNIFORM  
 COUPLED OPTICAL PATHS.....UNIFORM

WAVELENGTH (CM-1)	ADJACENT RESULTS (WATT/CM2*SP*CM-1)	ATMOSPHERIC TRANSMITTANCE	EFFECTIVE ATMOSPHERIC TRANSMITTANCE
ATMOSPHERE	SOURCE	SENSOR	
1.000E+03	0.000E+00	0.000E+00	0.000E+00
1.050E+03	0.000E+00	0.000E+00	0.000E+00
1.100E+03	0.000E+00	0.000E+00	0.000E+00
1.150E+03	0.000E+00	0.000E+00	0.000E+00
1.200E+03	0.000E+00	0.000E+00	0.000E+00
1.250E+03	0.000E+00	0.000E+00	0.000E+00
1.300E+03	0.000E+00	0.000E+00	0.000E+00
1.350E+03	0.000E+00	0.000E+00	0.000E+00
1.400E+03	0.000E+00	0.000E+00	0.000E+00
1.450E+03	0.000E+00	0.000E+00	0.000E+00
1.500E+03	0.000E+00	0.000E+00	0.000E+00
1.550E+03	0.000E+00	0.000E+00	0.000E+00
1.600E+03	0.000E+00	0.000E+00	0.000E+00
1.650E+03	0.000E+00	0.000E+00	0.000E+00
1.700E+03	0.000E+00	0.000E+00	0.000E+00
1.750E+03	0.000E+00	0.000E+00	0.000E+00
1.800E+03	0.000E+00	0.000E+00	0.000E+00
1.850E+03	0.000E+00	0.000E+00	0.000E+00
1.900E+03	0.000E+00	0.000E+00	0.000E+00
1.950E+03	0.000E+00	0.000E+00	0.000E+00
2.000E+03	0.000E+00	0.000E+00	0.000E+00
2.050E+03	0.000E+00	0.000E+00	0.000E+00
2.100E+03	0.000E+00	0.000E+00	0.000E+00
2.150E+03	0.000E+00	0.000E+00	0.000E+00
2.200E+03	0.000E+00	0.000E+00	0.000E+00
2.250E+03	0.000E+00	0.000E+00	0.000E+00
2.300E+03	0.000E+00	0.000E+00	0.000E+00
2.350E+03	0.000E+00	0.000E+00	0.000E+00
2.400E+03	0.000E+00	0.000E+00	0.000E+00
2.450E+03	0.000E+00	0.000E+00	0.000E+00
2.500E+03	0.000E+00	0.000E+00	0.000E+00
2.550E+03	0.000E+00	0.000E+00	0.000E+00
2.600E+03	0.000E+00	0.000E+00	0.000E+00
2.650E+03	0.000E+00	0.000E+00	0.000E+00
2.700E+03	0.000E+00	0.000E+00	0.000E+00
2.750E+03	0.000E+00	0.000E+00	0.000E+00
2.800E+03	0.000E+00	0.000E+00	0.000E+00
2.850E+03	0.000E+00	0.000E+00	0.000E+00
2.900E+03	0.000E+00	0.000E+00	0.000E+00
2.950E+03	0.000E+00	0.000E+00	0.000E+00
3.000E+03	0.000E+00	0.000E+00	0.000E+00
3.050E+03	0.000E+00	0.000E+00	0.000E+00
3.100E+03	0.000E+00	0.000E+00	0.000E+00
3.150E+03	0.000E+00	0.000E+00	0.000E+00
3.200E+03	0.000E+00	0.000E+00	0.000E+00
3.250E+03	0.000E+00	0.000E+00	0.000E+00
3.300E+03	0.000E+00	0.000E+00	0.000E+00
3.350E+03	0.000E+00	0.000E+00	0.000E+00
3.400E+03	0.000E+00	0.000E+00	0.000E+00
3.450E+03	0.000E+00	0.000E+00	0.000E+00
3.500E+03	0.000E+00	0.000E+00	0.000E+00
3.550E+03	0.000E+00	0.000E+00	0.000E+00
3.600E+03	0.000E+00	0.000E+00	0.000E+00
3.650E+03	0.000E+00	0.000E+00	0.000E+00
3.700E+03	0.000E+00	0.000E+00	0.000E+00
3.750E+03	0.000E+00	0.000E+00	0.000E+00
3.800E+03	0.000E+00	0.000E+00	0.000E+00
3.850E+03	0.000E+00	0.000E+00	0.000E+00
3.900E+03	0.000E+00	0.000E+00	0.000E+00
3.950E+03	0.000E+00	0.000E+00	0.000E+00
4.000E+03	0.000E+00	0.000E+00	0.000E+00
4.050E+03	0.000E+00	0.000E+00	0.000E+00
4.100E+03	0.000E+00	0.000E+00	0.000E+00
4.150E+03	0.000E+00	0.000E+00	0.000E+00
4.200E+03	0.000E+00	0.000E+00	0.000E+00
4.250E+03	0.000E+00	0.000E+00	0.000E+00
4.300E+03	0.000E+00	0.000E+00	0.000E+00
4.350E+03	0.000E+00	0.000E+00	0.000E+00
4.400E+03	0.000E+00	0.000E+00	0.000E+00

Figure 18. Output Listing for ERIM Case 9R with DR Approximation

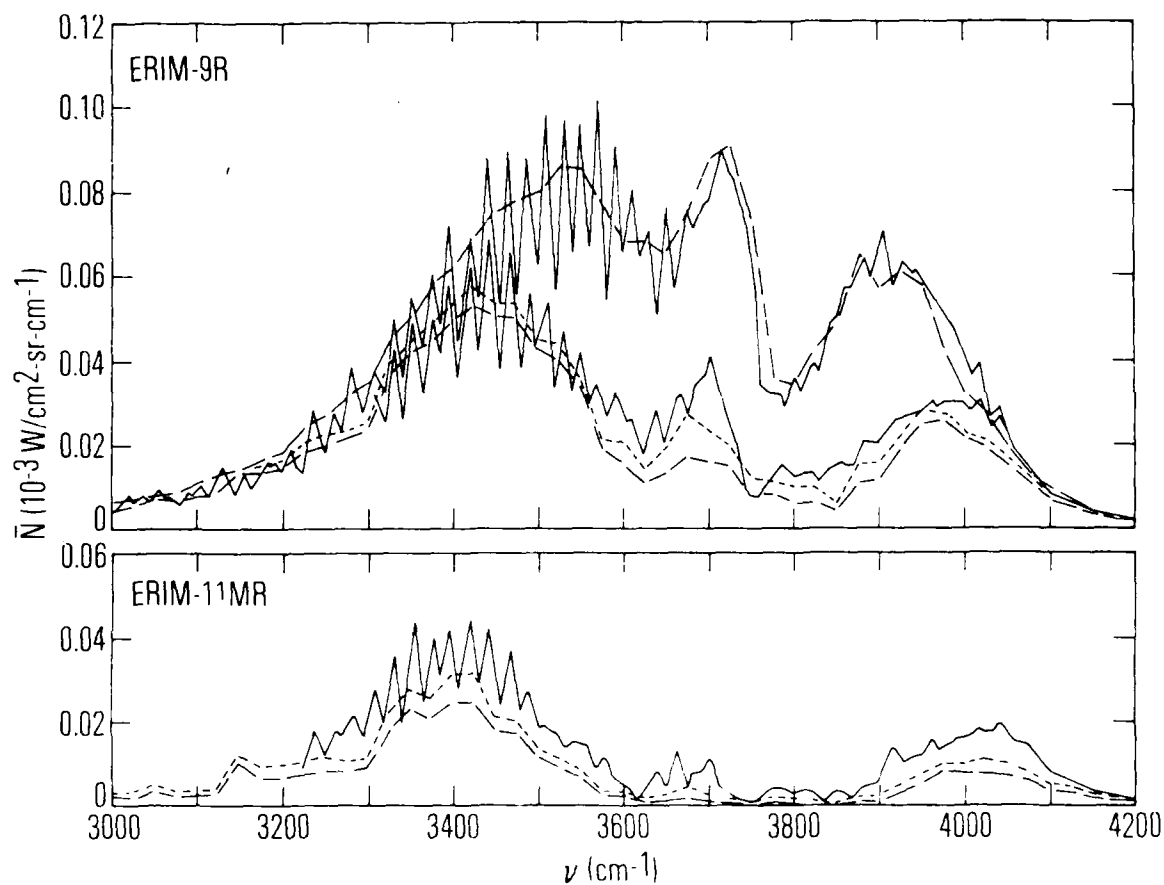


Figure 19. Comparison of Computed and Experimental Radiance Spectra for ERIM Hot-thru-Cold H<sub>2</sub>O Measurements. (a) ERIM 9R: \_\_\_\_\_ (upper) experimental source radiance; \_\_\_\_\_ (lower) experimental attenuated radiance; \_\_\_\_\_ (upper) computed source radiance; \_\_\_\_\_ (lower) computed attenuated radiance (CG approximation); ----- computed attenuated radiance (DR approximation). (b) ERIM 11 MR: \_\_\_\_\_ experimental attenuated radiance; \_\_\_\_\_ computed attenuated radiance (CG approximation); ----- computed attenuated radiance (DR approximation).

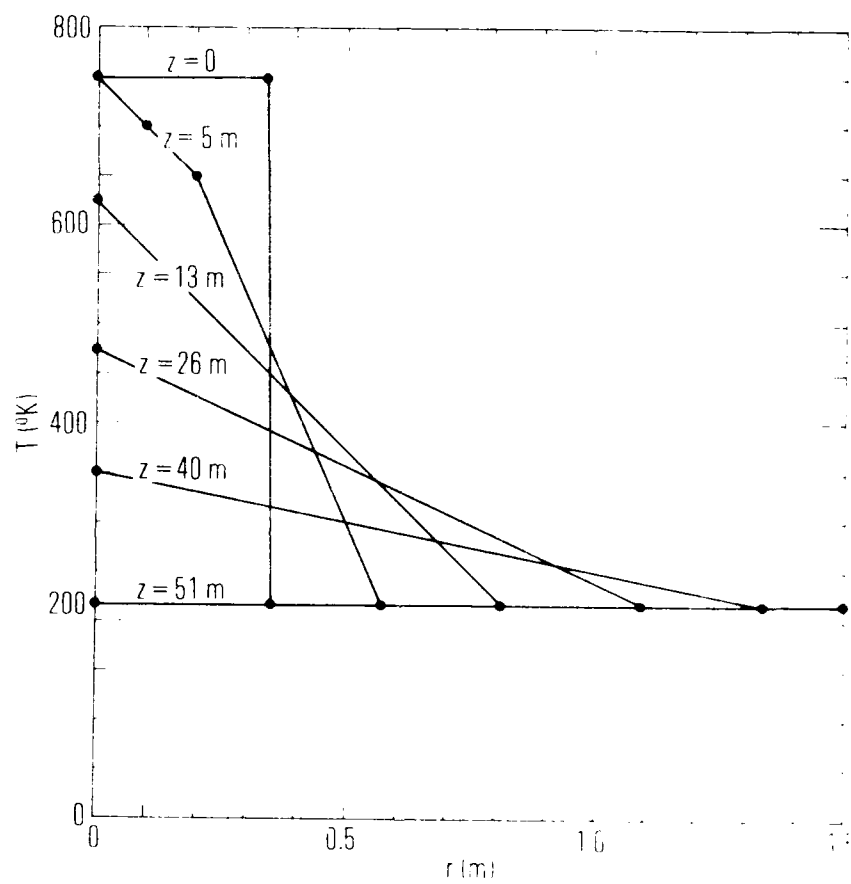


Figure 20. Plume Temperature Profiles

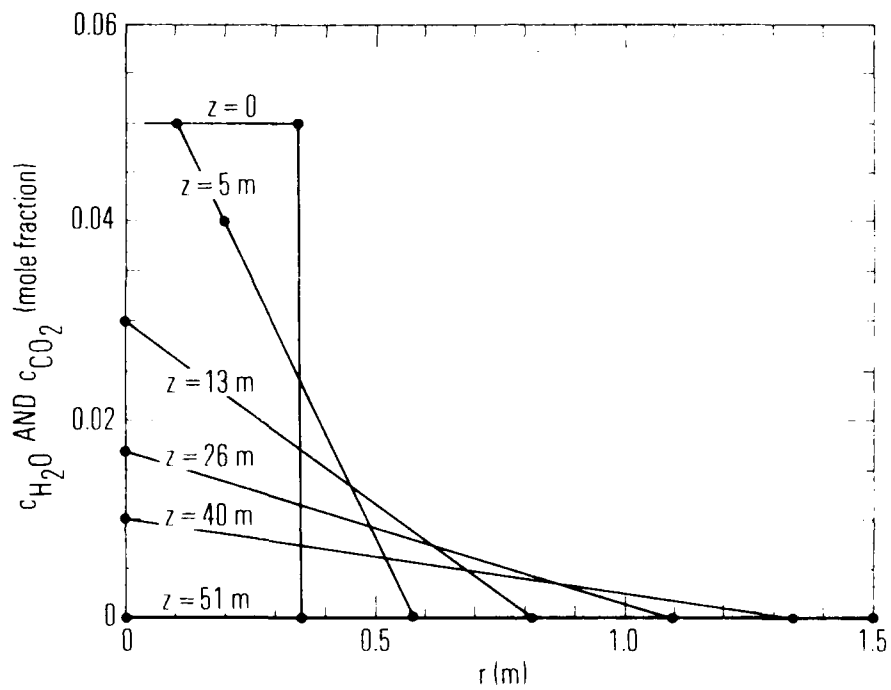


Figure 21. Plume Concentration Profiles

[illegible]

resolution in the 4.3- $\mu\text{m}$  region. Besides spectral results, in-band radiance values are calculated for two bandpasses in each of the two spectral regions. The bandpass limits encompass the red- and blue-spikes of the two spectral regions, and are tabulated in the input data listing of Figure 22.

Two viewing geometries are considered. The aircraft-to-aircraft geometry assumes a sensor located at the same altitude as the target plume and at a horizontal range of 2km. The atmospheric slant path is considered as a uniform absorption path. The space-to-aircraft geometry assumes a satellite-based sensor  $70^\circ$  off the target zenith. The atmosphere is assumed to terminate at 100km for this case. The portion of the atmosphere between the plume altitude (9.75km) and 100km is divided into 10 intervals of approximately each mass content. Non-uniformities along this slant path are handled with the CG approximation. For both viewing geometries, the atmospheric  $\text{H}_2\text{O}$  concentration of the McClatchey et al. <sup>(2)</sup> tropical model is used, and  $\text{CO}_2$  is assumed uniformly mixed with mixing ratio 0.000330. A broadside ( $\alpha = 90^\circ$ ) aspect is assumed for both cases.

By inspection of the plume profiles and the magnitude of the spectral absorption coefficients for  $\text{H}_2\text{O}$  and  $\text{CO}_2$ , it can be deduced that the plume is relatively optically thin throughout the spectral regions considered. The integration grid for the emission portion of the line of sight is chosen primarily to accommodate the degree of temperature and concentration gradient within the plume. The calculations are performed with an integration step size of  $\Delta s \approx 0.10\text{m}$  regardless of where the line of sight intersects the plume. Account of nonuniformities within the plume and that result from the coupling of the plume to the atmosphere is made with the DR approximation.

Before complete radiance calculations were made, an extensive mapping of the unattenuated plume radiance at the single spectral position  $\nu = 3700\text{ cm}^{-1}$  was made in order to define the extent and resolution of the area integration grid that would be required in order to perform

accurate integrations over the projected area of the plume. The integration grid tabulated in the input data listing of Figure 22 and pictured in Figure 23 was finally selected and verified to yield integration results accurate to approximately two percent (at  $3700\text{ cm}^{-1}$ ).

The input data deck for the final runs is listed in Figure 22. The first run covers the  $2.7\text{-}\mu\text{m}$  spectral region and the horizontal viewing geometry case. The second run redefines the viewing geometry only. The third run retains the space-sensor geometry of the second run, but redefines the spectral region and active species. The fourth run retains the  $4.3\text{-}\mu\text{m}$  spectral conditions, but reverts to the horizontal geometry. In all cases, a spatial map is made for the two bandpasses considered. The output listing of Figure 24 is limited to the aircraft-sensor geometry for the  $4.3\text{-}\mu\text{m}$  region and blue-spike bandpass  $2375 - 2400\text{ cm}^{-1}$ . The radiance and transmittance spectra for all of the runs are shown in Figures 25 through 27. Axial station and isoradiance contour plots derived (by hand) from the spatial distribution map of Figure 24 are shown in Figures 28 and 29, respectively.



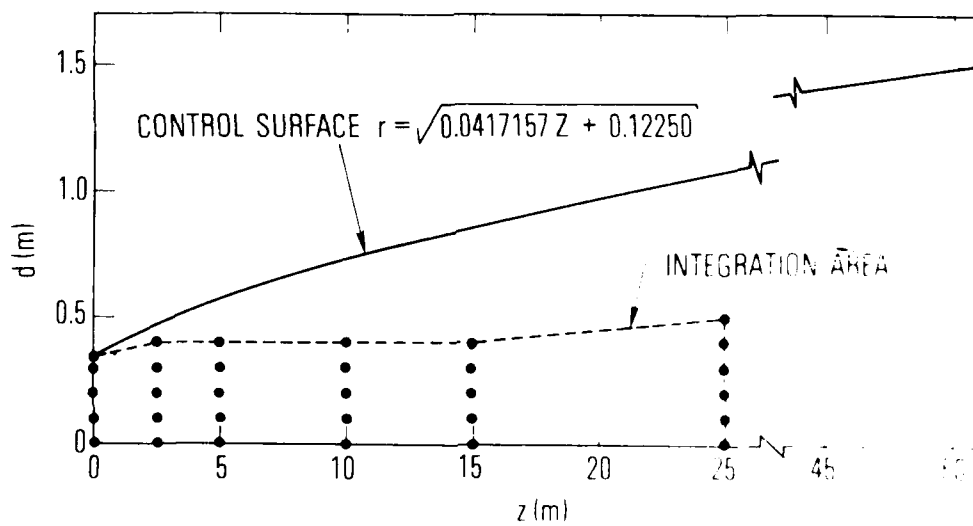


Figure 23. Projected Area Integration Grid



SPATIAL VARIATION OF BANDPASS AVERAGE RADIANCES OVER PROJECTED AREA OF PLUME

ASEFFECT ANGLE (DEG) 4.032E+01  
 CALCULATED DELTA (CM) 2.144E+02  
 BANDPASS 3375.00 TO 3400.00 CM-1

J	J(I)	IRADIANCE (W/CM <sup>2</sup> *S*CM-1)	TE
(METER)	SOURCE	SENSO-	
I= 1 Z(I)= 0.			
1	0.	5.524E-05	1.474E-01
2	1.000E-01	4.445E-05	1.464E-01
3	2.000E-01	4.607E-05	1.707E-01
4	3.000E-01	3.409E-05	1.453E-01
5	4.000E-01	0.	1.000E+00
STATION AVERAGES 4.177E-05 7.372E-06 1.765E-01			
I= 2 Z(I)= 2.500E+01			
1	0.	3.247E-05	2.064E-01
2	1.000E-01	3.443E-05	1.495E-01
3	2.000E-01	2.422E-05	1.788E-01
4	3.000E-01	1.134E-05	1.326E-01
5	4.000E-01	1.742E-04	1.163E-02
STATION AVERAGES 2.014E-05 3.744E-06 1.852E-01			
I= 3 Z(I)= 5.000E+01			
1	0.	2.244E-05	2.161E-01
2	1.000E-01	1.413E-05	2.003E-01
3	2.000E-01	2.470E-05	1.056E-01
4	3.000E-01	2.440E-05	1.077E-01
5	4.000E-01	3.644E-07	4.746E-02
STATION AVERAGES 1.009E-05 2.028E-06 1.897E-01			
I= 4 Z(I)= 1.000E+01			
1	0.	4.774E-06	1.745E-01
2	1.000E-01	7.657E-06	1.613E-01
3	2.000E-01	4.232E-06	1.109E-01
4	3.000E-01	1.664E-06	1.481E-02
5	4.000E-01	3.535E-07	5.398E-02
STATION AVERAGES 4.444E-06 7.104E-07 1.504E-01			
I= 5 Z(I)= 1.500E+01			
1	0.	4.414E-06	1.396E-01
2	1.000E-01	7.125E-06	1.204E-01
3	2.000E-01	1.405E-06	6.402E-02
4	3.000E-01	1.225E-07	7.704E-02
5	4.000E-01	1.677E-07	5.594E-02
STATION AVERAGES 2.044E-06 2.418E-07 1.154E-01			
I= 6 Z(I)= 2.000E+01			
1	0.	4.444E-07	4.614E-02
2	1.000E-01	7.170E-07	7.401E-02
3	2.000E-01	4.324E-07	2.003E-02
4	3.000E-01	2.454E-07	5.724E-02
5	4.000E-01	1.604E-07	4.544E-02
6	5.000E-01	7.941E-04	3.320E-02
STATION AVERAGES 4.744E-07 3.147E-04 7.351E-02			
PLUME AVERAGE 6.314E-06 1.170E-06 1.716E-01			

Figure 24. Output Listing for Jet-Plume Calculation in the 4.3- $\mu$ m Region with Aircraft-Sensor Geometry (sheet 2 of 2)

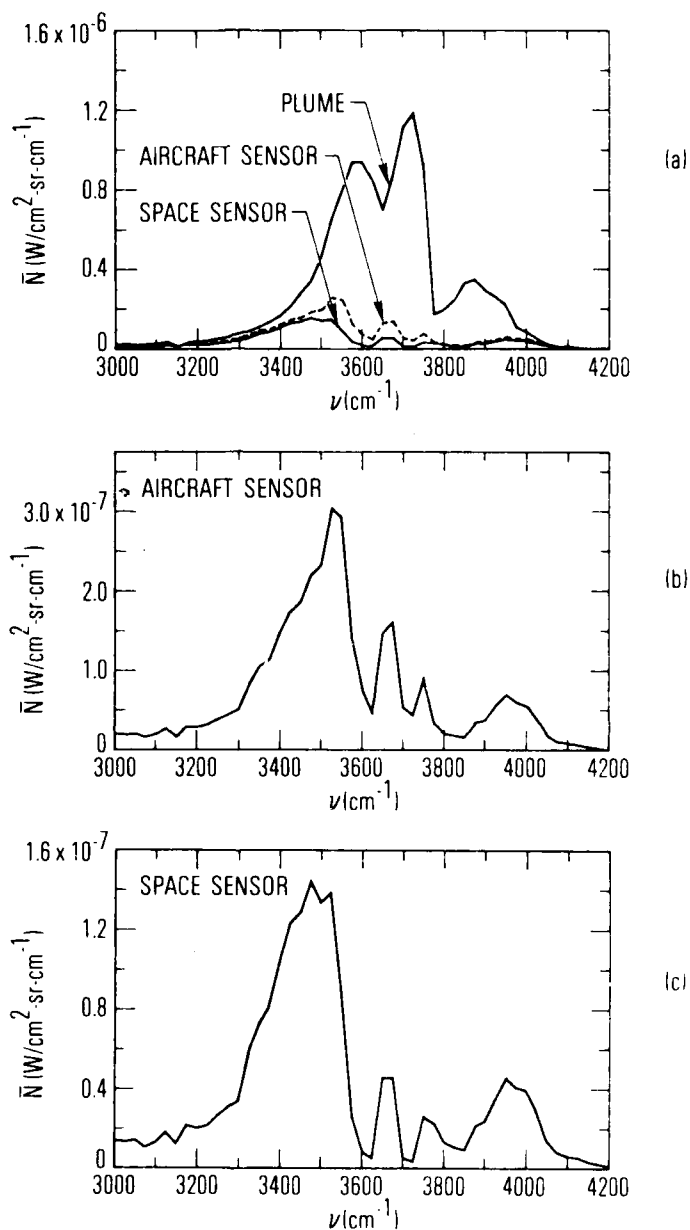


Figure 25. Radiance Spectra in 2.7- $\mu\text{m}$  Region. (a) Unattenuated and Attenuated Radiance for both Viewing Geometries. (b) Attenuated Radiance (expanded scale) for Aircraft-Sensor. (c) Attenuated Radiance (expanded scale) for Space-Sensor.

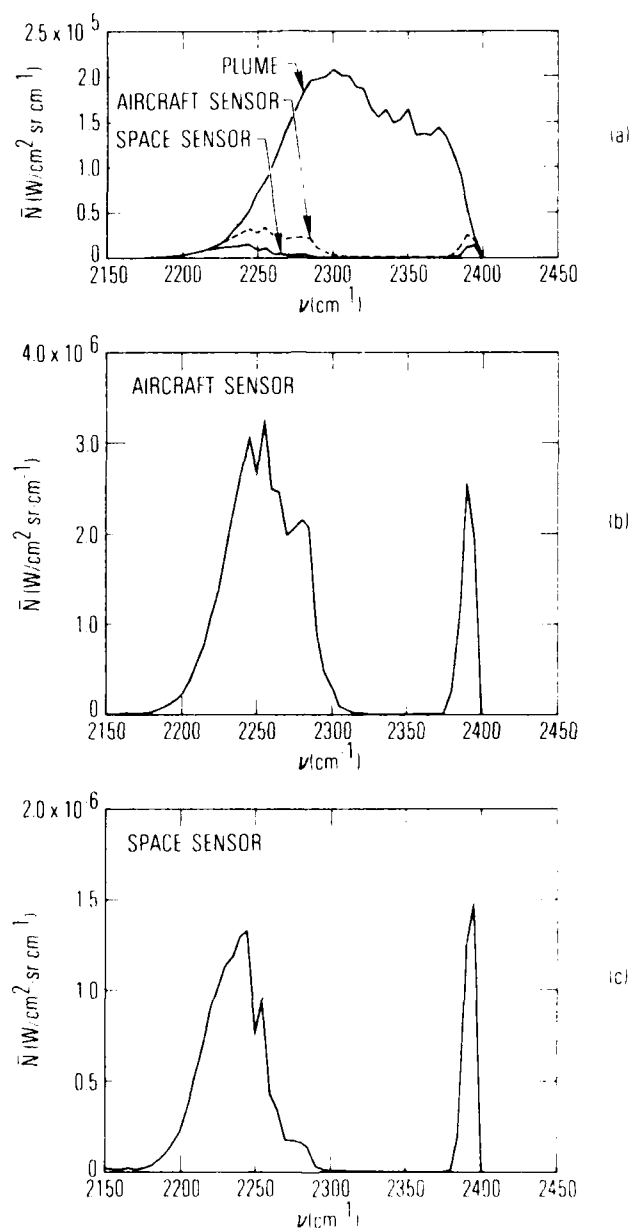


Figure 26. Radiance Spectra in 4.3- $\mu\text{m}$  Region. (a) Unattenuated and Attenuated Radiance for both Viewing Geometries. (b) Attenuated Radiance (expanded scale) for Aircraft-Sensor. (c) Attenuated Radiance (expanded scale) for Space-Sensor.

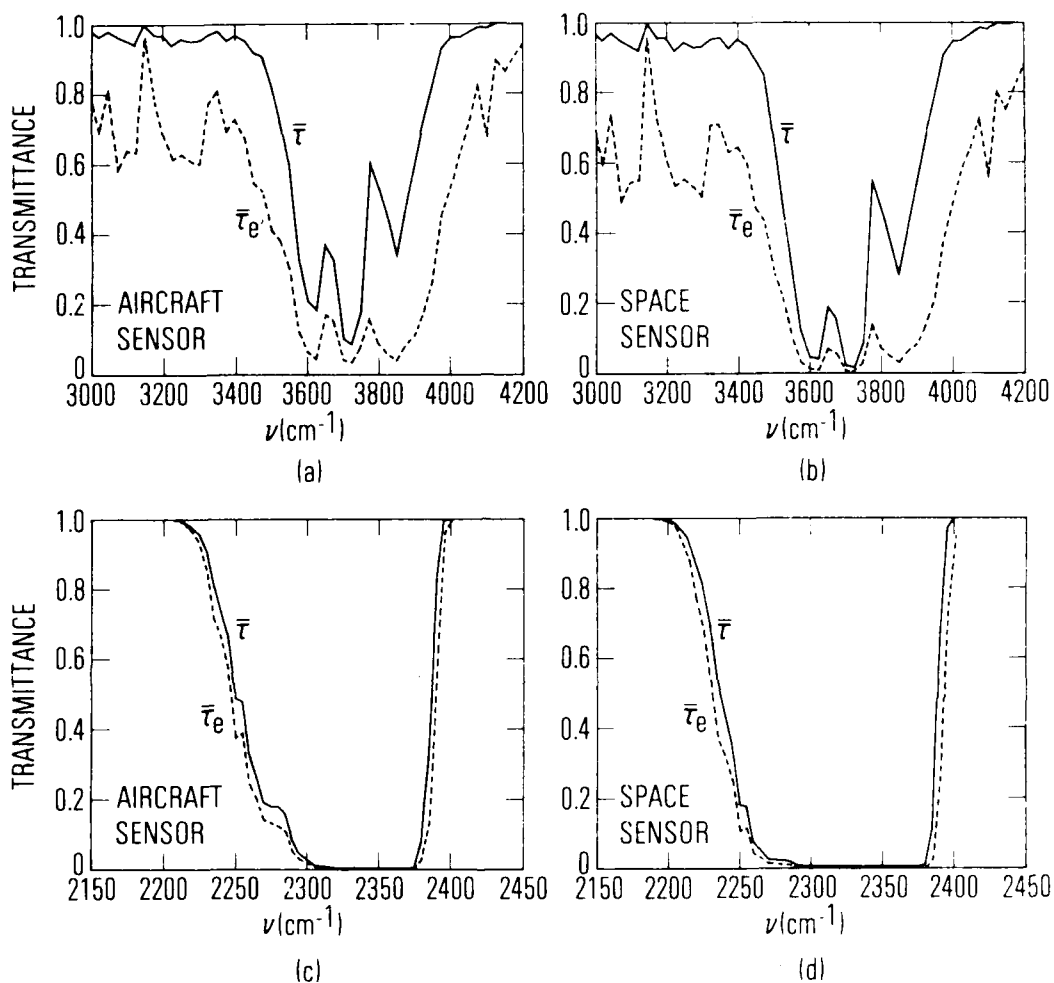


Figure 27. Atmospheric and Effective Atmospheric Transmittance Spectra. (a) Horizontal-Path, 2.7- $\mu\text{m}$  Region. (b) Slant-Path to Space, 2.7- $\mu\text{m}$  Region. (c) Horizontal-Path, 4.3- $\mu\text{m}$  Region. (d) Slant-Path to Space, 4.3- $\mu\text{m}$  Region.  $\bar{\tau}$  is the atmospheric transmittance for continuum radiation.  $\bar{\tau}_e$  is the effective atmospheric transmittance defined as the ratio of attenuated to unattenuated plume radiance.

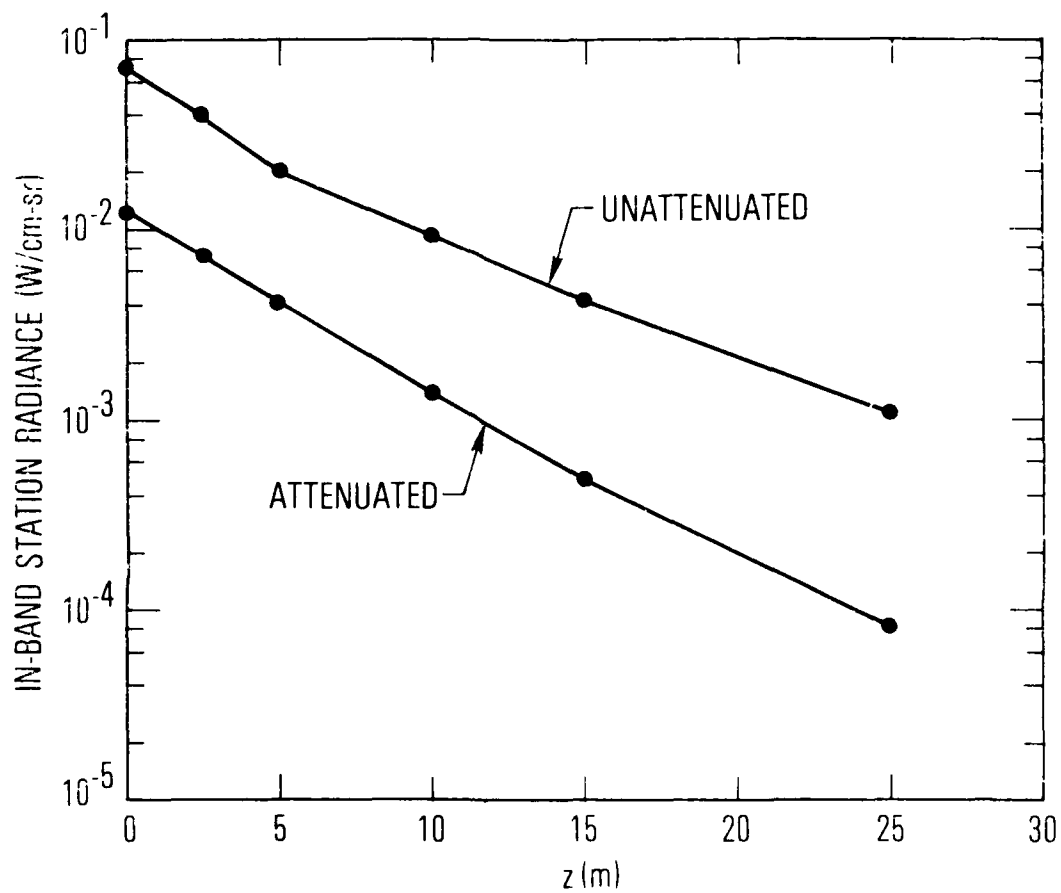


Figure 28. Axial-Station Variation of the 4.3- $\mu$ m Blue Spike Radiance for Aircraft-Sensor Geometry

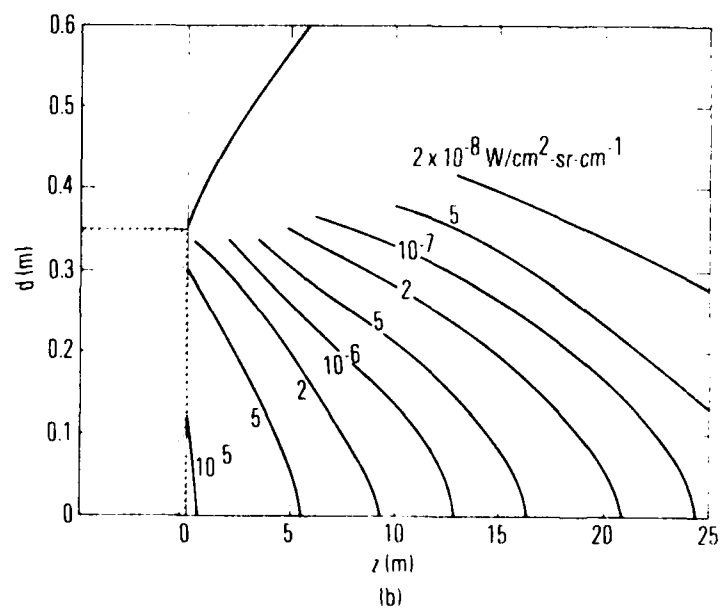
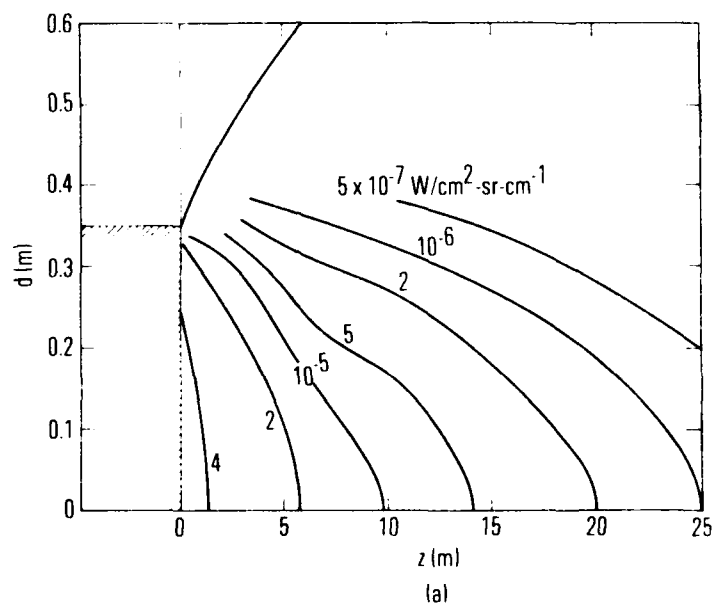


Figure 29. Isoradiance Contours of the 4.3- $\mu\text{m}$  Blue Spike Radiance for Aircraft-Sensor Geometry. (a) Unattenuated. (b) Attenuated.



## VI. CODE DISTRIBUTION

The code, band model parameters, and standard atmospheres are available on magnetic tape to interested users. (A blank tape must be supplied by the requestor.) The tape consists of 80 column card images blocked at 60 cards per block, and can be supplied either as a 9-track tape with EBCDIC coded characters or as a 7-track tape with BCD coded characters. Any of the commonly available bit densities can be accommodated. The tape is divided into 17 partitions separated by end-of-file marks. The first partition is the FORTRAN source deck for the code. The next 10 partitions are the band model parameter sets of Table 2. The last six partitions of the tape are the standard model atmospheres of Table 1. Each of the 10 band model parameter partitions corresponds to the card deck structure of Figure 12, and each of the six atmosphere partitions corresponds to the card deck structure of Figure 13 (with IUNIT  $\neq$  1). An input deck of control cards and auxiliary data decks corresponding to a limited version of example B of Section V will be supplied, as well as the results of a job run made directly with this deck and the user's tape.

The code is written for the CDC 7600 computer with SCOPE2 operating system. The following information is given to facilitate the adaptation of the code to other systems.

1. Small Core Memory Requirement:  $125642_8$  words (This includes the requirements for subroutine SPLOT and the Aerospace in-house plotting routines,  $6307_8$  words).
2. Large Core Memory Requirements:  $203720_8$  words.
3. Computer memory must be preset to zero.
4. All Hollerith variables and constants are 10 characters long.
5. Input and output devices must be defined to be consistent with the following FORTRAN statements:

READ (5, format number) .... card input (e.g., control card deck).

WRITE (6, format number) .... printer listing

READ (2, format number) .... band model parameters

READ (3, format number) .... standard atmospheres

Although the code has been used and checked on many test cases, the author cannot guarantee that the coding is completely error free, and in fact, would appreciate notification of errors found by users.

## REFERENCES

1. A. J. LaRocca and R. E. Turner, Atmospheric Transmittance and Radiance: Methods of Calculation, 107600-10-T, Environmental Research Institute of Michigan, Ann Arbor, Mich. (June 1975).
2. R. A. McClatchey, R. W. Fenn, J. E. A. Selby, F. E. Volz and J. S. Garing, Optical Properties of the Atmosphere (Revised), AFCRL-71-0279, Air Force Geophysics Laboratories, Bedford, Mass. (10 May 1971).
3. C. B. Ludwig, W. Malkmus, J. E. Reardon and J. A. L. Thompson, Handbook of Infrared Radiation from Combustion Gases, eds. R. Goulard and J. A. L. Thompson, NASA SP-3080, Marshall Space Flight Center, Huntsville, Ala. (1973).
4. R. A. McClatchey, W. S. Benedict, S. A. Clough, D. E. Burch, R. F. Calfe, K. Fox, L. S. Rothman and J. S. Garing, AFCRL Atmospheric Absorption Line Parameters Compilation, AFCRL-TR-73-006, Air Force Geophysics Laboratories, Bedford, Mass. (25 January 1973).
5. S. J. Young, Band Model Parameters for the 2.7- $\mu$ m Bands of H<sub>2</sub>O and CO<sub>2</sub> in the 100 to 3000°K Temperature Range, TR-0076 (6970)-4, The Aerospace Corporation, El Segundo, Calif. (31 July 1975).
6. S. J. Young, Band Model Parameters for the 4.3- $\mu$ m Fundamental Band of CO<sub>2</sub> in the 100-3000°K Temperature Range, TR-0076 (6754-03)-1, The Aerospace Corporation, El Segundo, Calif. (19 February 1976).
7. S. J. Young, "Band Model Formulation for Inhomogeneous Optical Paths", J. Quant. Spectros. Radiat. Transfer, **15**, 483-501 (1975).
8. S. J. Young, "Addendum to: Band Model Formulation for Inhomogeneous Optical Paths", J. Quant. Spectros. Radiat. Transfer, **15**, 1137-1140 (1975).
9. S. J. Young, Band Model Calculation of Atmospheric Transmittance for Hot Gas Line Emission Sources. Account of Doppler Broadening, TR-0076(6970)-5, The Aerospace Corporation, El Segundo, Calif. (30 July 1975).
10. S. J. Young, "Nonisothermal Band Model Theory", submitted to J. Quant. Spectros. Radiat. Transfer, (1976).

#### REFERENCES (Continued)

11. C. D. Rodgers and A. P. Williams, "Integrated Absorption of a Spectral Line with the Voigt Profile", J. Quant. Spectros. Radiat. Transfer, 14, 319-323 (1974).
12. G. H. Lindquist, C. B. Arnold and R. L. Spellicy, Atmospheric Absorption Applied to Plume Emission: Experimental and Analytical Investigations of Hot Gas Emission Attenuated by Cold Gases, 102700-20-F, Environmental Research Institute of Michigan, Ann Arbor, Mich. (August 1975).
13. S. J. Young, "Evaluation of Nonisothermal Band Models for  $H_2O$ ", submitted to J. Quant. Spectros. Radiat. Transfer, (1976).

### THE IVAN A. GETTING LABORATORIES

The Laboratory Operations of The Aerospace Corporation is conducting experimental and theoretical investigations necessary for the evaluation and application of scientific advances to new military concepts and systems. Versatility and flexibility have been developed to a high degree by the laboratory personnel in dealing with the many problems encountered in the nation's rapidly developing space and missile systems. Expertise in the latest scientific developments is vital to the accomplishment of tasks related to these problems. The laboratories that contribute to this research are:

Aerophysics Laboratory: Launch and reentry aerodynamics, heat transfer, reentry physics, chemical kinetics, structural mechanics, flight dynamics, atmospheric pollution, and high-power gas lasers.

Chemistry and Physics Laboratory: Atmospheric reactions and atmospheric optics, chemical reactions in polluted atmospheres, chemical reactions of excited species in rocket plumes, chemical thermodynamics, plasma and laser-induced reactions, laser chemistry, propulsion chemistry, space vacuum and radiation effects on materials, lubrication and surface phenomena, photo-sensitive materials and sensors, high precision laser ranging, and the application of physics and chemistry to problems of law enforcement and biomedicine.

Electronics Research Laboratory: Electromagnetic theory, devices, and propagation phenomena, including plasma electromagnetics; quantum electronics, lasers, and electro-optics; communication sciences, applied electronics, semiconducting, superconducting, and crystal device physics, optical and acoustical imaging; atmospheric pollution; millimeter wave and far-infrared technology.

Materials Sciences Laboratory: Development of new materials; metal matrix composites and new forms of carbon; test and evaluation of graphite and ceramics in reentry; spacecraft materials and electronic components in nuclear weapons environment; application of fracture mechanics to stress corrosion and fatigue-induced fractures in structural metals.

Space Sciences Laboratory: Atmospheric and ionospheric physics, radiation from the atmosphere, density and composition of the atmosphere, aurorae and airglow; magnetospheric physics, cosmic rays, generation and propagation of plasma waves in the magnetosphere; solar physics, studies of solar magnetic fields; space astronomy, x-ray astronomy; the effects of nuclear explosions, magnetic storms, and solar activity on the earth's atmosphere, ionosphere, and magnetosphere; the effects of optical, electromagnetic, and particulate radiations in space on space systems.

THE AEROSPACE CORPORATION  
El Segundo, California